

Review

Natural Aerosols, Gaseous Precursors and Their Impacts in Greece: A Review from the Remote Sensing Perspective

Vassilis Amiridis ^{1,*}, Stelios Kazadzis ^{2,3}, Antonis Gkikas ⁴, Kalliopi Artemis Voudouri ^{1,5}, Dimitra Kouklaki ^{1,6}, Maria-Elissavet Koukouli ⁵, Katerina Garane ⁵, Aristeidis K. Georgoulias ⁷, Stavros Solomos ⁴, George Varlas ⁸, Anna Kampouri ¹, Dimitra Founda ³, Basil E. Psiloglou ³, Petros Katsafados ⁹, Kyriakoula Papachristopoulou ¹, Ilias Fountoulakis ^{1,4}, Panagiotis-Ioannis Raptis ³, Thanasis Georgiou ^{1,10}, Anna Gialitaki ^{1,11}, Emmanouil Proestakis ¹, Alexandra Tsekeri ¹, Eleni Drakaki ¹, Eleni Marinou ¹, Elina Giannakaki ¹², Stergios Misios ⁴, John Kapsomenakis ⁴, Kostas Eleftheratos ^{6,13}, Nikos Hatzianastassiou ¹⁴, Pavlos Kalabokas ⁴, Prodromos Zanis ⁷, Mihalis Vrekoussis ^{15,16,17}, Alexandros Papayannis ^{18,19}, Andreas Kazantzidis ²⁰, Konstantinos Kourtidis ²¹, Dimitris Balis ⁵, Alkiviadis F. Bais ⁵ and Christos Zerefos ^{4,6,22,23}

¹ Institute for Astronomy, Astrophysics, Space Applications and Remote Sensing, National Observatory of Athens, 152 36 Athens, Greece; kavoudou@noa.gr (K.A.V.); d.kouklaki@noa.gr (D.K.); akampouri@noa.gr (A.K.); kpapachr@noa.gr (K.P.); ifountoulakis@academyofathens.gr (I.F.); ageorgiou@noa.gr (T.G.); togialitaki@noa.gr (A.G.); proestakis@noa.gr (E.P.); atsekeri@noa.gr (A.T.); eldrakaki@noa.gr (E.D.); elmarinou@noa.gr (E.M.)

² Physikalisch-Meteorologisches Observatorium Davos, World Radiation Center, Dorfstrasse 33, Davos, 7260 Dorf, Switzerland; stelios.kazadzis@pmodwrc.ch

³ Institute for Environmental Research and Sustainable Development, National Observatory of Athens, Palaia Penteli, 152 36 Athens, Greece; founda@noa.gr (D.F.); bill@noa.gr (B.E.P.); piraptis@noa.gr (P.-I.R.)

⁴ Research Centre for Atmospheric Physics and Climatology, Academy of Athens, 106 79 Athens, Greece; agkikas@academyofathens.gr (A.G.); ssolomos@academyofathens.gr (S.S.); smisios@academyofathens.gr (S.M.); jkaps@academyofathens.gr (J.K.); pkalabokas@academyofathens.gr (P.K.); zerefos@academyofathens.gr (C.Z.)

⁵ Laboratory of Atmospheric Physics, School of Physics, Aristotle University of Thessaloniki, 541 24 Thessaloniki, Greece; mariliza@auth.gr (M.-E.K.); agarane@auth.gr (K.G.); balis@auth.gr (D.B.); abais@auth.gr (A.F.B.)

⁶ Department of Geology and Geoenvironment, National and Kapodistrian University of Athens, 115 27 Athens, Greece; kelef@geol.uoa.gr

⁷ Department of Meteorology and Climatology, School of Geology, Aristotle University of Thessaloniki, 541 24 Thessaloniki, Greece; ageor@auth.gr (A.K.G.); zanis@geo.auth.gr (P.Z.)

⁸ Hellenic Centre for Marine Research, Institute of Marine Biological Resources and Inland Waters, 46.7 km of Athens-Sounio Ave., 190 13 Anavissos, Greece; gvarlas@hcmr.gr

⁹ Department of Geography, Harokopio University of Athens, 176 76 Athens, Greece; pkatsaf@hua.gr

¹⁰ School of Physics, Aristotle University of Thessaloniki, 541 24 Thessaloniki, Greece

¹¹ Department of Physics and Astronomy, Earth Observation Science Group, University of Leicester, Leicester LE1 7RH, UK

¹² Department of Environmental Physics and Meteorology, Faculty of Physics, National and Kapodistrian University of Athens, 115 27 Athens, Greece; elina@phys.uoa.gr

¹³ Biomedical Research Foundation, Academy of Athens, 115 27 Athens, Greece

¹⁴ Laboratory of Meteorology, Department of Physics, University of Ioannina, 451 10 Ioannina, Greece; nhatzian@uoii.gr

¹⁵ Institute of Environmental Physics (IUP), University of Bremen, 28359 Bremen, Germany; mvrekous@uni-bremen.de

¹⁶ Center of Marine Environmental Sciences (MARUM), University of Bremen, 28359 Bremen, Germany

¹⁷ Climate and Atmosphere Research Center (CARE-C), The Cyprus Institute, Nicosia 2121, Cyprus

¹⁸ Laser Remote Sensing Unit (LRSU), Physics Department, National Technical University of Athens, 157 80 Zografou, Greece; aplidar@mail.ntua.gr

¹⁹ Laboratory of Atmospheric Processes and Their Impacts, School of Architecture, Civil and Environmental Engineering, École Polytechnique Fédérale de Lausanne, 1003 Lausanne, Switzerland

²⁰ Laboratory of Atmospheric Physics, Department of Physics, University of Patras, 265 00 Patras, Greece; akaza@upatras.gr

²¹ Department of Environmental Engineering, Democritus University of Thrace, 671 00 Xanthi, Greece; kourtidi@env.duth.gr

²² Navarino Environmental Observatory (N.E.O.), 240 01 Messinia, Greece



Citation: Amiridis, V.; Kazadzis, S.; Gkikas, A.; Voudouri, K.A.; Kouklaki, D.; Koukouli, M.-E.; Garane, K.; Georgoulias, A.K.; Solomos, S.; Varlas, G.; et al. Natural Aerosols, Gaseous Precursors and Their Impacts in Greece: A Review from the Remote Sensing Perspective. *Atmosphere* **2024**, *15*, 753. <https://doi.org/10.3390/atmos15070753>

Academic Editor: Davide Zanchettin

Received: 22 May 2024

Revised: 18 June 2024

Accepted: 19 June 2024

Published: 24 June 2024



Copyright: © 2024 by the authors. Licensee MDPI, Basel, Switzerland. This article is an open access article distributed under the terms and conditions of the Creative Commons Attribution (CC BY) license (<https://creativecommons.org/licenses/by/4.0/>).

²³ Mariolopoulos-Kanaginis Foundation for the Environmental Sciences, 106 75 Athens, Greece
* Correspondence: vamoir@noa.gr

Abstract: The Mediterranean, and particularly its Eastern basin, is a crossroad of air masses advected from Europe, Asia and Africa. Anthropogenic emissions from its megacities meet over the Eastern Mediterranean, with natural emissions from the Saharan and Middle East deserts, smoke from frequent forest fires, background marine and pollen particles emitted from ocean and vegetation, respectively. This mixture of natural aerosols and gaseous precursors (Short-Lived Climate Forcers—SLCFs in IPCC) has short atmospheric residence times but strongly affects radiation and cloud formation, contributing the largest uncertainty to estimates and interpretations of the changing cloud and precipitation patterns across the basin. The SLCFs' global forcing is comparable in magnitude to that of the long-lived greenhouse gases; however, the local forcing by SLCFs can far exceed those of the long-lived gases, according to the Intergovernmental Panel on Climate Change (IPCC). Monitoring the spatiotemporal distribution of SLCFs using remote sensing techniques is important for understanding their properties along with aging processes and impacts on radiation, clouds, weather and climate. This article reviews the current state of scientific know-how on the properties and trends of SLCFs in the Eastern Mediterranean along with their regional interactions and impacts, depicted by ground- and space-based remote sensing techniques.

Keywords: short-lived climate forcers; Mediterranean

1. Introduction

Observing SLCFs [1] over the Eastern Mediterranean is of importance because their concentrations are typically 2- to 10-times higher than in the hemispheric background troposphere [2]. There has been a significant number of studies on SLCF abundance, properties, and spatiotemporal distributions and trends over Greece and the extended Eastern Mediterranean in the last 20 years, utilizing ground- and satellite-based remote sensors.

Satellite remote sensing has been utilized to study the SLCF spatiotemporal distributions over the greater Eastern Mediterranean region, based on data from Meteosat [3], SeaWiFS (e.g., [4]), TOMS (e.g., [5–9]), MODIS Terra and Aqua (e.g., [6–8,10–26]), OMI/AURA (e.g., [8,9,27]), CALIOP/CALIPSO (e.g., [28–30]), MISR/Terra (e.g., [31]), as well as NOAA/AVHRR, MERIS/ENVISAT, AATSR/ENVISAT, PARASOL/POLDER, MSG/SEVIRI and Landsat satellite observations (e.g., [32,33]). Ground-based remote sensors have also been used to study the aerosol and trace gas abundance and characterization over Greece, utilizing sensors, such as lidars (e.g., [34–56]), MAX-DOAS ([57–62]), sun photometers (e.g., [48,63–69]), Brewer spectrophotometers (e.g., [6,65,70–75]), Multi-Filter Radiometers (e.g., [76–78]) and ceilometers (e.g., [79,80]). In addition to the systematic ground-based observations [81], a number of experimental campaigns have been conducted in the last few decades in Greece, supported by the PANhellenic infrastructure for Atmospheric Composition and climatE chAnge (PANACEA) National Research Infrastructure (the Greek component of the Aerosol, Clouds and Trace Gases Research Infrastructure—ACTRIS European Research Infrastructure), to address specific science objectives of interest. A list of the recent experiments includes the Pre-TECT ([82]) experiment in Finokalia focusing on desert dust characterization and the CALISHTO experiment in Helmos for aerosol–cloud interactions ([83]).

This article is structured as follows: the current state of scientific know-how on the properties and trends of the natural aerosols and the gaseous precursors over the Mediterranean is described in Section 1. Section 2 describes their regional interactions and impacts as, depicted by ground- and space-based remote sensing techniques. Finally, Section 3 contains the summary and main recommendations for future research.

1.1. Natural Aerosols

1.1.1. Aerosol Types and Sources

The diversity of aerosol species that we see in Greece (Figure 1) results from the convergence of air masses carrying aerosols from natural sources situated in the surrounding regions (e.g., [84,85]). Residing in the proximity of the Sahara Desert, Greece receives massive amounts of mineral dust particles, mainly in spring and summer [8,30,86]. Smoke from local forest fires also plays a critical role in the accumulation of light-absorbing soot particles in summer [87–89]. Transboundary smoke advection over Greece from sources in Ukraine, Portugal, the Balkans and Canada has also been reported [22,44,51,54,69,90–94]. Volcanic particles (composed of ash and sulphates) constitute another natural aerosol component affecting Greece after Etna or Icelandic volcanic eruptions [42,47,95–98]. Among the recorded aerosol species, a significant contribution results from marine particles produced by bursting bubbles during whitecap formation, attributed to wind–wave interactions (e.g., [99]). Biogenic particles consisting mainly of airborne fungi and pollen grains also contribute to the natural aerosol burden in the Greek area [100–104].

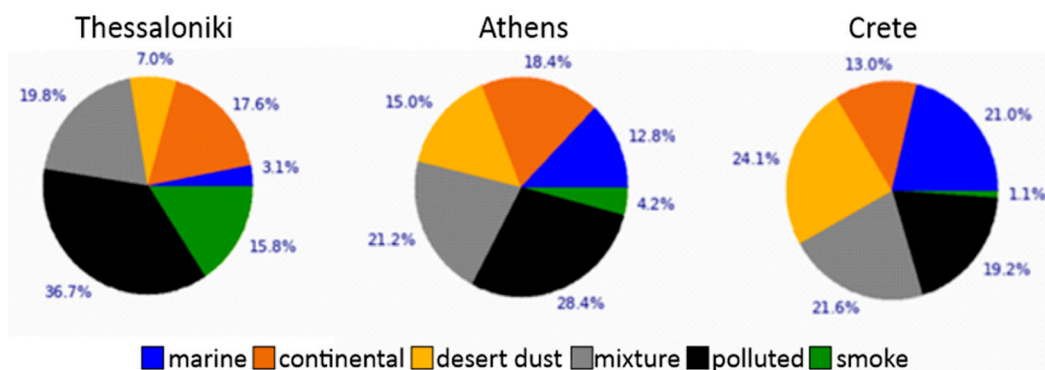


Figure 1. Columnar climatological estimation of the aerosol types observed in Thessaloniki, Athens and Crete, as retrieved from the AErosol RObotic NETwork (AERONET) data. Based on OPAC ([105,106], source: [107]).

1.1.2. Current Knowledge Per Aerosol Type

Desert Dust: Dust outbreaks frequently affect the broader Greek region, as revealed by passive and active remote sensing techniques. On a seasonal basis, dust optical depths (DODs) are maximized in spring, when cyclonic pressure systems, inducing south–southwesterly winds, favor the advection of Saharan mineral particles towards Greece [9,21,77]. Similar airmass pathways are recorded in winter [108], whereas during summer months, dust-laden air masses, originating in the north-western parts of the Sahara, carry mineral particles over Greece after crossing the Italian peninsula [30,37,39–41,43]. Under favorable conditions (i.e., dust sources activation, strong winds, weak removal mechanisms), DODs can yield extreme values (>2) [8,109,110], with the core portion of the dust burden residing up to 6 km, while mineral particles at low concentrations are detected up to 10 km [30,111,112]. Such extreme events take place about 9 days/year (mainly in spring) in the southern parts of Greece (Crete), while their frequency drops down to 1–2 days/year in the north [8,111]. Dust has been shown to account for about one-third of the total aerosol optical depth (AOD) over Greece using satellite observations from the Moderate-Resolution Imaging Spectroradiometer (MODIS) and reanalysis/model data [23,26]. Based on the MIDAS dust dataset (2003–2017, [15]), the most negative trends over the extended Greek area are computed in summer and spring (down to−0.010/year) ([24]; Figure 2). The zonal distribution of the dust extinction vertical distribution from CALIPSO-LIVAS dust product [113] for the region 20°–30° E for the latitudinal region from 10°–60° N is depicted in Figure 2 (seasonal distribution [30]).

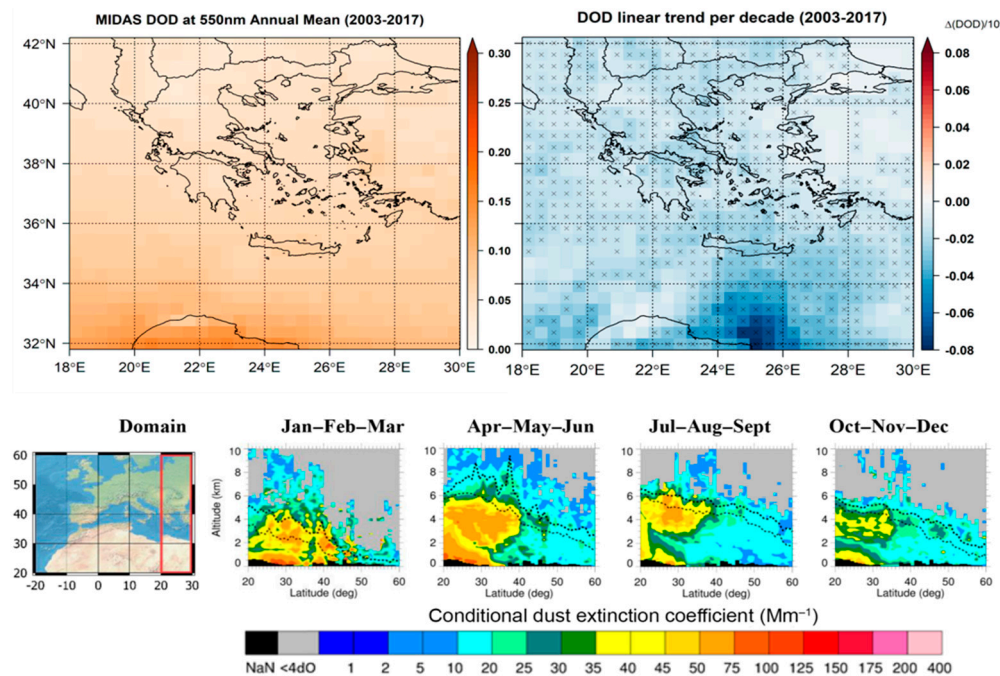


Figure 2. (Upper left): Annual mean dust optical depth (DOD) at 550 nm from MIDAS (2003–2017); (upper right): trends (statistically significant at 95% confidence level) of deseasonalized DOD from MIDAS (2003–2017); (lower) zonal seasonal distribution of the conditional dust extinction vertical distribution from CALIPSO–LIVAS dust product.

A more comprehensive description of dust optical and microphysical properties is depicted by ground-based lidars and sun photometers operating in Greece, providing vertically resolved and columnar information, respectively (e.g., [5,35,39,41–43,45,49,63,68,69,79,114–120]). Among other conclusions, the aforementioned studies reveal the following: dust outbreaks cause exceptional exceedances of AOD levels (>0.3) and reductions in the Ångström exponent (<0.5); dust layers are mainly confined between 1.5 and 6.5 km a.s.l. over Greece; the irregular shape and the large dust particle size led to significantly high depolarization values (~30%) and medium lidar ratio values (~45 sr).

Fire Smoke: Smoke from local forest fires and across Eastern Europe developed under dry conditions, and strong winds play a critical role in the accumulation of light-absorbing soot particles in summer [75,87–89]. Although originating from medium-strength fires, these intense smoke plumes usually penetrate the Planetary Boundary Layer (PBL) to reach the free troposphere (e.g., [90]). This is possible due to the complex Greek topography and the interchange between land and marine boundary layers and also due to convective processes and Pyro-Cb formation [121,122]. The dispersion of smoke from wildfires over Greece is detected and forecasted by the Firehub-smoke platform ([123,124]; Figure 3).

Smoke detections over Greece from distant sources include the plumes from biomass burning of agricultural waste in Eastern Europe and grassland/shrubland fires along the coasts of the Black Sea [44,50,92,94,125–129], Portugal wildfires [122], and Canadian wildfires [51,54,69,93,118]. The studies report that the smoke particles were found to be relatively small, with high Ångström exponents and high lidar ratios (of the order of 70 ± 20 sr) due to their absorption and size distribution [22,45,55,120,127,128]. Siomos et al. [48] report AOD values at 355 nm ranging from 0.18 to 0.24, with the exception of summer in the free troposphere, where the largest AOD value occurs (~0.4). The observed variability in smoke properties is attributed to the particle age, which affects the absorption efficiency and particle hygroscopic growth processes (e.g., [44]). For the same reasons, large variability in the depolarization ratio of smoke has been reported (e.g., [128,129]) due to particle age or the particle water uptake due to different humidity conditions. Gialitaki et al. [54] shows, however, that for the Canadian stratospheric smoke observed above Europe in August 2017,

the observed depolarization and lidar ratio values (along with their spectral dependence) can be successfully reproduced with a proposed model of compact near-spherical particles.

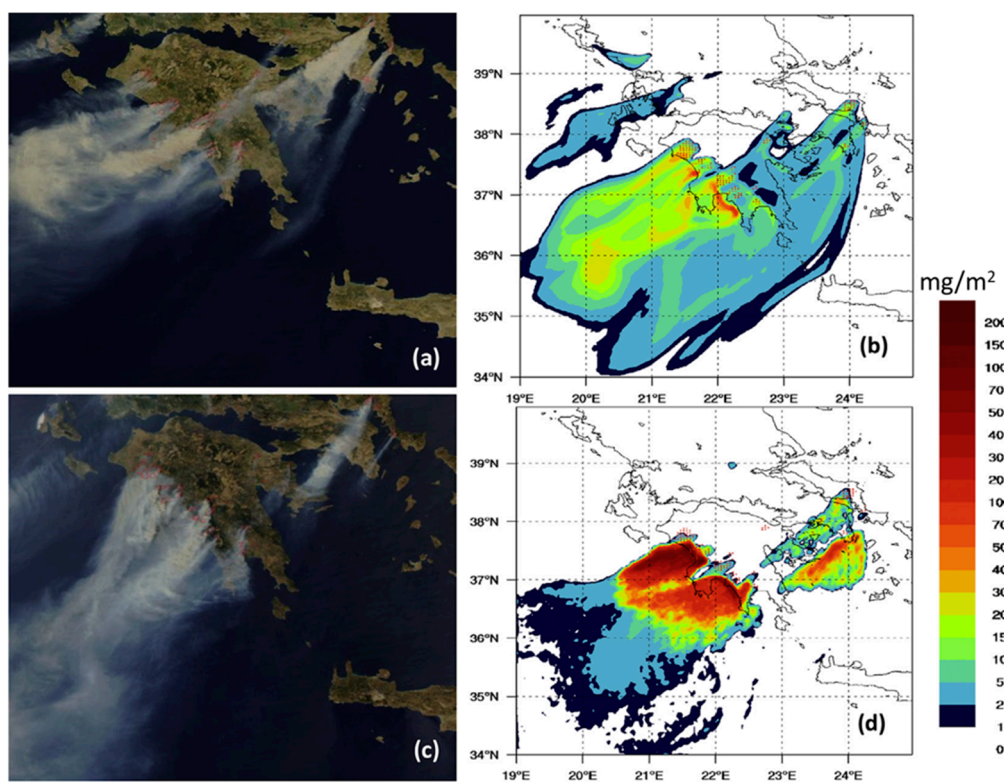


Figure 3. (a) MODIS image on 25 August 2007 20:00 UTC; (b) column concentration of smoke (mg/m^2) from a concurrent FLEXPART-FireHub simulation; (c) MODIS image on 26 August 2007 09:30 UTC; (d) column concentration of smoke (mg/m^2) from a concurrent FLEXPART-Fire.

Marine: Marine aerosols are a major component of natural aerosols, especially in countries surrounded by sea, such as Greece (e.g., [99]). Georgoulias et al. [22] reports that marine aerosols account for about one-fourth of the total AOD over the Greek seas. The two main processes responsible for the formation of marine sea-spray droplets are: (1) the bursting of air bubbles in whitecaps, which releases film and jet sea-spray droplets, and (2) the direct tearing of spume sea-spray droplets from the edges of breaking waves [130]. The ejected sea-spray droplets evaporate when they enter a drier atmospheric environment, releasing sea-salt particles that circulate in the atmosphere and, finally, drop back to the surface through dry and wet deposition [131]. Sea-salt particles feature a predominant coarse mode and are spherical under humid conditions. Haarig et al. [132] report that the marine particle depolarization ratio shows a strong increase (up to 10%) during the phase transition from spherical sea-salt particles to cubic-like sea-salt crystals under low relative humidities in the marine boundary layer (below 50%). However, the lidar ratio shows very small variability, within 20–25 sr for all states.

During the last decade, the monitoring of sea-salt particles in Greece with ground-based remote sensing instruments that operated during the CHARADMEExp and Pre-TECT campaigns in Finokalia and PANGEA stations provided critical datasets for constraining modeled emissions [117,133,134]. As presented by Varlas et al. [99], the consideration of wind–wave interactions in models drives towards a better agreement with observations, mainly due to the increase in emissions at low-to-moderate wind intensities. Varlas et al. [99] corroborated Regayre et al. [135], who suggested that the default sea-spray emissions in wind-only-dependent models need to be increased by a factor of approximately three when wind speeds are relatively low. However, they have to be reduced in winter (usually characterized by relatively higher winds). The convergence of the two

studies strengthens the aspect that there is a necessity of revisiting sea-spray emissions by reconsidering the dependence of sea-salt aerosol emissions on the wind regime, while also designing more complete modeling methods, including not only wind speed but also physical processes such as waves and white capping.

Volcanic aerosols: Volcanic eruptions can inject large amounts of volcanic ash and gases (e.g., sulfur dioxide, SO_2) into the atmosphere, which can influence the radiation budget and climate [136], ecosystems, agriculture and aviation but even air quality and health [137–142]. Greece is often affected by the long-range transport of volcanic aerosols, mainly due to continuous Etna volcanic activity. Mt. Etna is the largest point source of particulate matter in the atmosphere of the Mediterranean, affecting the atmospheric levels of airborne particles and their deposition rates at both local and regional scales [97,98,143,144]. The optical properties of volcanic ash aerosols are generally similar to those of desert dust, as shown by Wang et al. [145] and Ansmann et al. [146] for fresh ash, with particle linear depolarization ratios reaching 0.37 and lidar ratio at 532 nm of 50–65 sr. Aged volcanic particles transported over Greece from the Icelandic volcano eruption of 2010 indicate lower depolarization ratios of 0.1–0.25 and lidar ratios for 355 nm within the range 55–70 sr [42,147]. Fresh volcanic ash plumes injected from Etna are systematically recorded in the PANGEA observatory. The plumes usually travel at free tropospheric heights, while WRF-FLEXPART forecasts of the projected pathways, constrained by satellite and PANGEA observations, are provided by NOA (Figure 4; [97]). Occasional transport over Greece of volcanic aerosols at stratospheric heights can also occur (e.g., [53,84]).

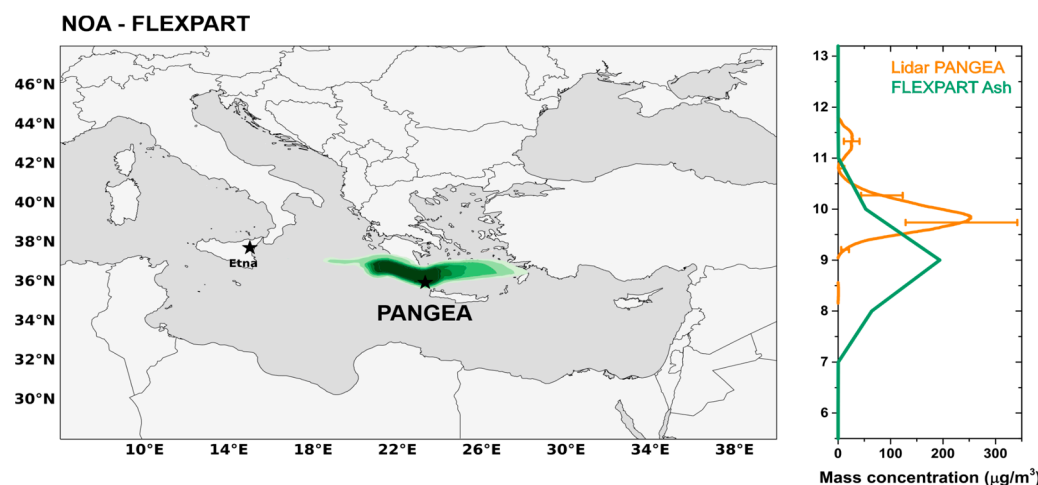


Figure 4. FLEXPART simulations of the volcanic ash columnar concentrations ($\mu\text{g}/\text{m}^{-2}$) originating from Etna, transported over Greece, using meteorological fields with Aeolus wind assimilation (12 March 2021, 19:30 UTC). (Right): Ash mass concentrations calculated by the PANGEA depolarization lidar (orange) and modeled with FLEXPART (green).

Pollen: Pollen is an essential part of plant reproduction as it stores and transports the genetic information of the plant. Pollen grains transferred by winds have various effects on climate and human health (e.g., [148,149]). Pollen can be lifted to several kilometers by turbulent mixing within the boundary layer and above and, thus, transported by wind over thousands of kilometers [150–153]. Dispersed in the atmosphere, they can affect the climate by acting as ice nucleation and cloud condensation nuclei, promoting the formation of clouds [154–158]. In the Mediterranean region, olive (*Olea europaea*) pollen is considered as one of the most important causes of respiratory allergic disease, whereas cypress (*Cupressus*) releases enormous amounts of anemophilous pollen and has been recognized to be responsible for a significant portion of the overall airborne pollen [159]. Recently, an increasing interest in pollen has arisen in the aerosol lidar community. Bohlmann et al. [160] showed that in the absence of other non-spherical particles, light detection and ranging (lidar) measurements and especially the particle

depolarization ratio can be used to track pollen grains in the atmosphere. However, the atmospheric aerosol population is always a mixture of several particle types and, thus, identifying pure pollen optical properties is still difficult. Shang et al. [161] reported that the depolarization ratio at 532 nm for pure birch (*Betula*) was in the order of 25% and 35% for pine pollen. Airborne pollen measurements in the Mediterranean region were performed at Finokalia station in Crete to characterize the optical properties of pollen. The linear particle depolarization ratio of pollen was relatively small, with a maximum of 0.15, since the shape of the majority of pollen types in the region is quasi-spherical.

1.2. Gaseous Precursors

Ground-based and satellite remote sensing has been used for the monitoring and evaluation of NO₂, total and tropospheric ozone, methane and SO₂ levels in the Mediterranean, as discussed in the following.

Total Ozone: The study of ozone variations in Greece started in the early 1980s, using ground-based measurements from Dobson [162] and Brewer spectrophotometers, along with various satellite missions (e.g., [163–170] etc.) and allowed for the detection of signs of the ozone layer depletion over Thessaloniki and Athens in the 1980s and the 1990s. The associated changes in solar UV-B radiation were also analyzed (e.g., [171–173]). More recent studies investigated longer-term measurements of total ozone in Thessaloniki, Greece [174–177] and detected a non-significant increase in total ozone between 1997 and mid-2010, likely associated with ozone recovery [178]. In Figure 5, the time series of the monthly mean departures (in percent) of total ozone from the climatological means are shown for Thessaloniki for the period 1982–2024. Total ozone measurements for this figure were performed by the first commercially available Brewer spectrophotometer, serial number #005, which is a single monochromator type MKII operating at the Laboratory of Atmospheric Physics [179], Thessaloniki, since 1982 and regularly calibrated via its systematic participation in international intercomparison campaigns. The analysis revealed a sharp decrease in stratospheric ozone in the early 1990s, which was attributed to the effect of the Mt. Pinatubo volcanic eruption. The 41-year record shows that total ozone has a statistically significant overall negative trend of -0.6% per decade, driven by the strong negative change of -3.8% per decade until 1996. Since then, the ozone layer record at Thessaloniki has been recovering at a (non-statistically significant) slower rate of -0.2% per decade.

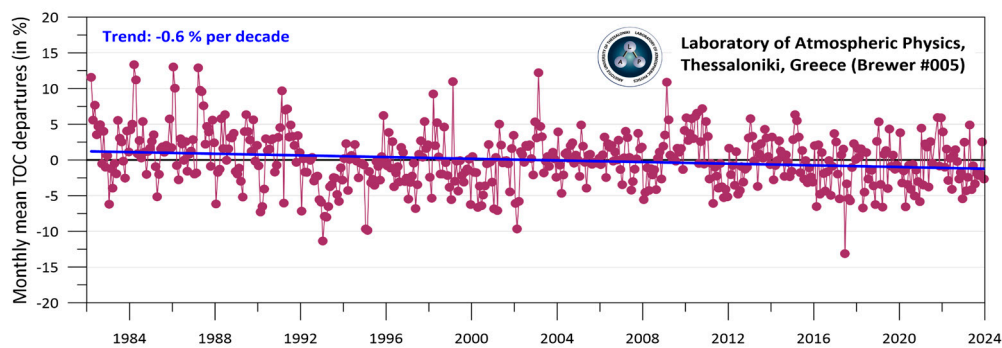


Figure 5. Monthly mean percentage departures from the climatological values of total ozone and the respective estimated trend, retrieved by the Brewer spectrophotometer #005, operating in Thessaloniki since 1982.

Eleftheratos et al. [180] analyzed the ground-based Brewer measurements of total ozone in the urban environment of Athens for the period July 2003–July 2019 and estimated a 16-year climatological mean of total ozone of about 322 Dobson Units (DU), with no significant change since 2003. An update of the data until July 2023 confirmed these findings.

The high-quality ground-based measurements of total ozone that are performed on a daily basis in Athens and Thessaloniki are used to systematically validate satellite-based ozone retrieving instruments that provide larger spatial coverage than the ground-based observations (e.g., [181–183]).

Tropospheric Ozone: The inter-connectivity of tropospheric O_3 and aerosol direct effects is manifold; on one hand, the increased presence of aerosols reduces radiation reaching the ground, and the subsequent photolysis reduction can decrease tropospheric O_3 in polluted areas during summer. On the other hand, enhanced aerosol presence leads to cooling, which suppresses atmospheric ventilation and results in increased surface-level O_3 in wintertime [184]. The Eastern Mediterranean is among the regions with the highest levels of background tropospheric ozone worldwide [185]. Three atmospheric processes controlling its formation in the region, namely the long-range transport of polluted air masses, the dynamic subsidence at mid-tropospheric levels and the stratosphere-to-troposphere exchange, have been extensively studied for the region (e.g., [186–190]). Recent space-borne observations have shown that in the Mediterranean troposphere, between the surface and 2 km, O_3 is mostly formed from anthropogenic emissions, while above 4 km, it is mostly transported from outside the domain or from stratospheric origins [191].

In Figure 6, the seasonal summertime mean observations of surface O_3 by AIRS/Aura are presented, for the daytime observations in the left and the nighttime observations in the right. The mean daytime surface O_3 spans between 50 and 66 ppb, with a mean of 55 ± 8 ppb, while the nighttime exhibits lower levels, between 44 and 56 ppb, with a mean of 53 ± 6 ppb for the whole region shown in this figure.

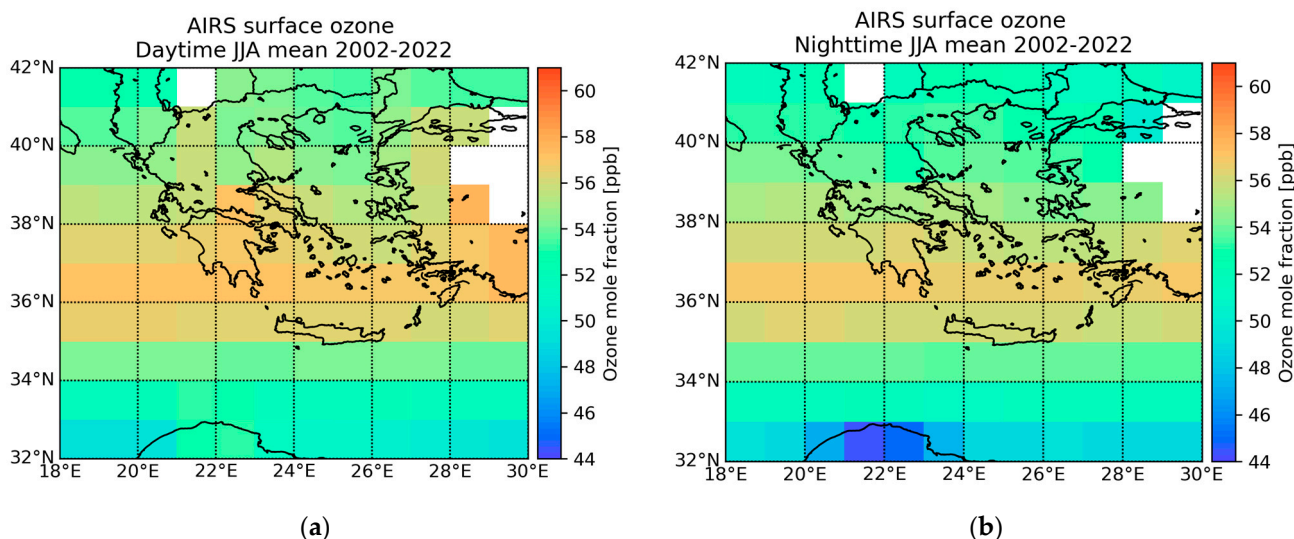


Figure 6. AIRS/Aura seasonal summertime mean surface O_3 vmr levels [ppb] over the Eastern Mediterranean from 2002 to 2022. (a) Daytime and (b) nighttime observations. Data acquired from ([192]).

Methane: The study of methane variations over the Eastern Mediterranean, including Greece, was initially based on 2003–2004 data from SCIAMACHY on ENVISAT [193]. A summer–autumn peak was observed for both 2003 and 2004, August being the month with the highest methane concentrations. Recently, Kourtidis et al. [194] used 2018–2022 data from the Tropospheric Monitoring Instrument (TROPOMI) on Sentinel 5P (S5P) to study methane concentrations over the greater Thessaloniki area. They found increased concentrations over the rice fields of Chalastra, biological waste treatment units and biogas plants, and garbage burial sites.

Since early 2019, methane levels over Thessaloniki and the surrounding areas are monitored via the Bruker EM27/SUN ground-based low-resolution Fourier-Transform spectrometer operated according to the requirements of the Collaborative Carbon Column Observing Network (COCCON) in the Laboratory of Atmospheric Physics, Aristotle University of Thessaloniki [195]. In a recent study, based on four years of observations, the methane levels were found to have increased by approximately 4%, with the highest concentrations of ~1.92 ppm during early 2022 [196]. Excellent agreement was also reported against collocated TROPOMI/S5P observations, with a mean of $-0.01 \pm 0.6\%$, underlying the significance of satellite measurements as a valuable supplement to ground-based data for the purpose of greenhouse gas monitoring.

In Figure 7, the monthly mean methane levels over the Eastern Mediterranean based on the Atmospheric Infrared Sounder (AIRS) on board the Aura satellite are presented. A very pronounced positive trend of ~5 ppb per annum is found for the timeframe 2012 to 2023, alongside a stable seasonal pattern, with a peak-to-peak amplitude of $\pm 15.5 \pm 2.5$ ppb. According to the latest European State of the Climate report [197], the annual increase in atmospheric concentrations for methane has been about 9 ppb/year (0.5%/year) since 2010, with the growth rates being larger than 10 ppb/year in the last three years, with a record high growth rate of about 17 ppb/year in 2021.

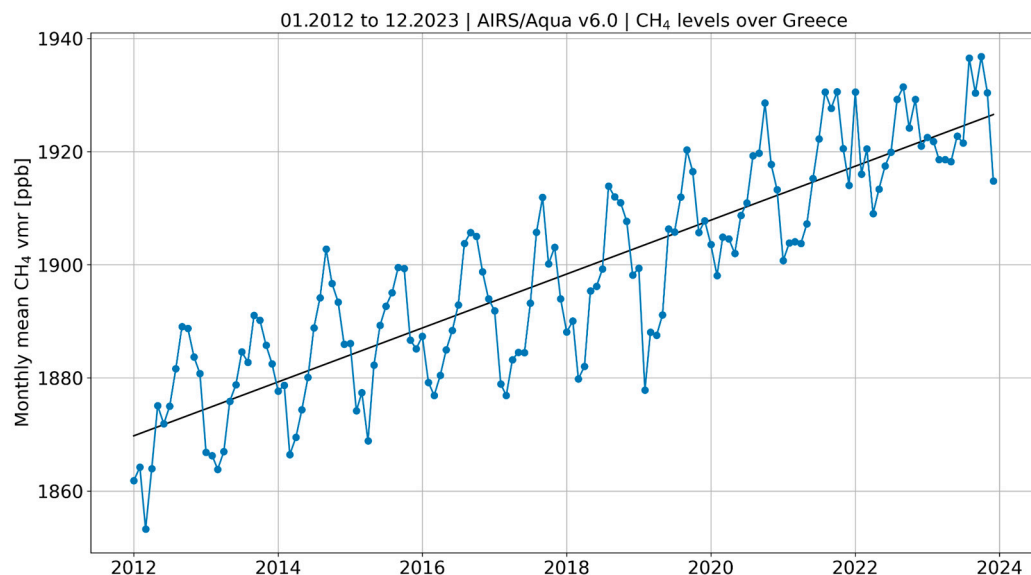


Figure 7. AIRS/Aura monthly mean CH₄ vmr levels [ppb] over the Eastern Mediterranean from 01.2012 to 12.2023. Data acquired from ([198]).

Nitrogen dioxide: Recent studies have unequivocally shown the ability of space-borne air quality observations to monitor both long-term and short-term changes in NO_x emissions over Greece while also identifying the specific emission sector [199–202]. These observations also revealed the adverse results of the 2008–2010 economic crisis on air quality over Greek urban sites [203,204], reflecting the reduction in traffic activity due to economic factors in Greek cities and the subsequent drop in oil consumption. For Athens, Georgoulias et al. [205], using multi-satellite data, showed that tropospheric NO₂ stabilized after 2010 following a consistent decline in the preceding years (1996–2010), with a rate of $-1.76\% \text{ yr}^{-1}$. On the contrary, for Greece as a whole, the tropospheric NO₂ trend reversed from positive ($0.52\% \text{ yr}^{-1}$) to strongly negative ($-4.22\% \text{ yr}^{-1}$) after 2012, according to the same study. Recently, Alexandri et al. [206], using satellite NO₂ observations from a single sensor (OMI/AURA), indicated strong decreasing trends over various locations in Greece over the fifteen-year period of 2005–2019 (e.g., $-3.95\% \text{ yr}^{-1}$ for Kozani, $-3.57\% \text{ yr}^{-1}$ for Athens and $-2.89\% \text{ yr}^{-1}$ for Thessaloniki). The implementation of lockdown measures subsequent to the 2020 outbreak of COVID-19 resulted in abrupt alterations to nitrogen

dioxide emissions across Greece. Monthly mean tropospheric nitrogen dioxide (NO_2) observations showed an average decrease of 15% and 11% for March and April 2020, respectively, compared with the previous year, over the six larger Greek metropolitan areas, mostly attributable to vehicular emission reductions [207]. The ability of space-borne observations to quantify and monitor changes in nitrogen oxide (NO_x) emissions over Northwestern Greece, where four lignite-burning power plants are located, was investigated by Skoulidou et al. [202]. Mean decreases of about –35% and –63% in NO_x emissions are estimated for the two larger power plants in the summers of 2018 and 2019, respectively, supported by similar decreases in the reported energy production of the power plants (~–30% and –70%, respectively).

In Figure 8 we report on the improvement in air quality over Greece as observed by the OMI/Aura sensor measuring tropospheric NO_2 levels. In the upper left panel, the mean 2005–2010 tropospheric NO_2 vertical column densities show the high levels over Athens, Thessaloniki as well as the Ptolemaida power plant in the Northwest of the country. In the upper right, based on the mean 2015–2020 levels, a marked decrease is reported for all high emitting locations. In the lower panel, the absolute difference plot between the multi-annual means of 2005–2010 and 2015–2020 further demonstrates the decline in NO_2 emissions in recent times.

Ground-based observations of NO_2 are being systematically performed in both Athens and Thessaloniki. Drosoglou et al. [57] placed three multi-axial differential optical absorption spectroscopy (MAX-DOAS) systems at different sites, representing urban, suburban and rural conditions around Thessaloniki. They found that the average measured tropospheric NO_2 was $\sim 12.0 \pm 7.5 \times 10^{15}$ molecules cm^{-2} for the center of Thessaloniki, whereas the mean values for the suburban and rural sites were $\sim 6.0 \pm 3.5 \times 10^{15}$ and $\sim 5.0 \pm 2.5 \times 10^{15}$ molecules cm^{-2} , respectively. In the recent work of Karagkiozidis et al. [208], employing an upgraded MAX-DOAS system, these urban gradients were confirmed, further reporting a “weekend effect”, with approximately 30% lower NO_2 concentrations at weekends compared to working days. For the urban Athens area, Gratsea et al. [59–61] also presented tropospheric NO_2 columns derived from ground-based MAX-DOAS observations, clearly identifying seasonal variability with lower NO_2 levels in summer, highly correlated ($r \approx 0.85$) with the urban background and suburban in situ observations. In Drosoglou et al. [209], five years of total, tropospheric and near-surface NO_2 observations from a Pandora spectrometer system, routinely operating in the city center of Athens, Greece, were presented for the first time, further revealing a clear weekly pattern with low NO_2 concentrations on Sundays, while a diurnal cycle with higher levels of NO_2 in the morning was observed from the ground due to the high NO_x emissions from heavy traffic in the urban environment.

Sulfur dioxide: Satellite observations have been used to monitor anthropogenic SO_2 emissions since 1995, while Zerefos et al. (2000) identified enhanced SO_2 over Southeastern Europe, attributed to lignite combustion in local power plants, with 50% of the observed SO_2 column over Northern Greece attributable to lignite-burning sources in Bulgaria, Romania and former Yugoslavia, using GOME/ERS-2 observations. Georgoulias et al. [210] studied ground- and space-borne observations of the sulfur load over Thessaloniki. From 1983 to 2006, the SO_2 levels above Thessaloniki generally decreased, with ~ 0.03 DU per annum, due to the European Union’s strict sulfur control policies on vehicular emissions. They also found that the seasonal variability in the SO_2 total column exhibits a double-peak structure with two maxima, one during winter and the second during summer. The winter peak can be attributed to central heating, while the summer peak is due to synoptic transport from sources west of the city and sources in the north of Greece.

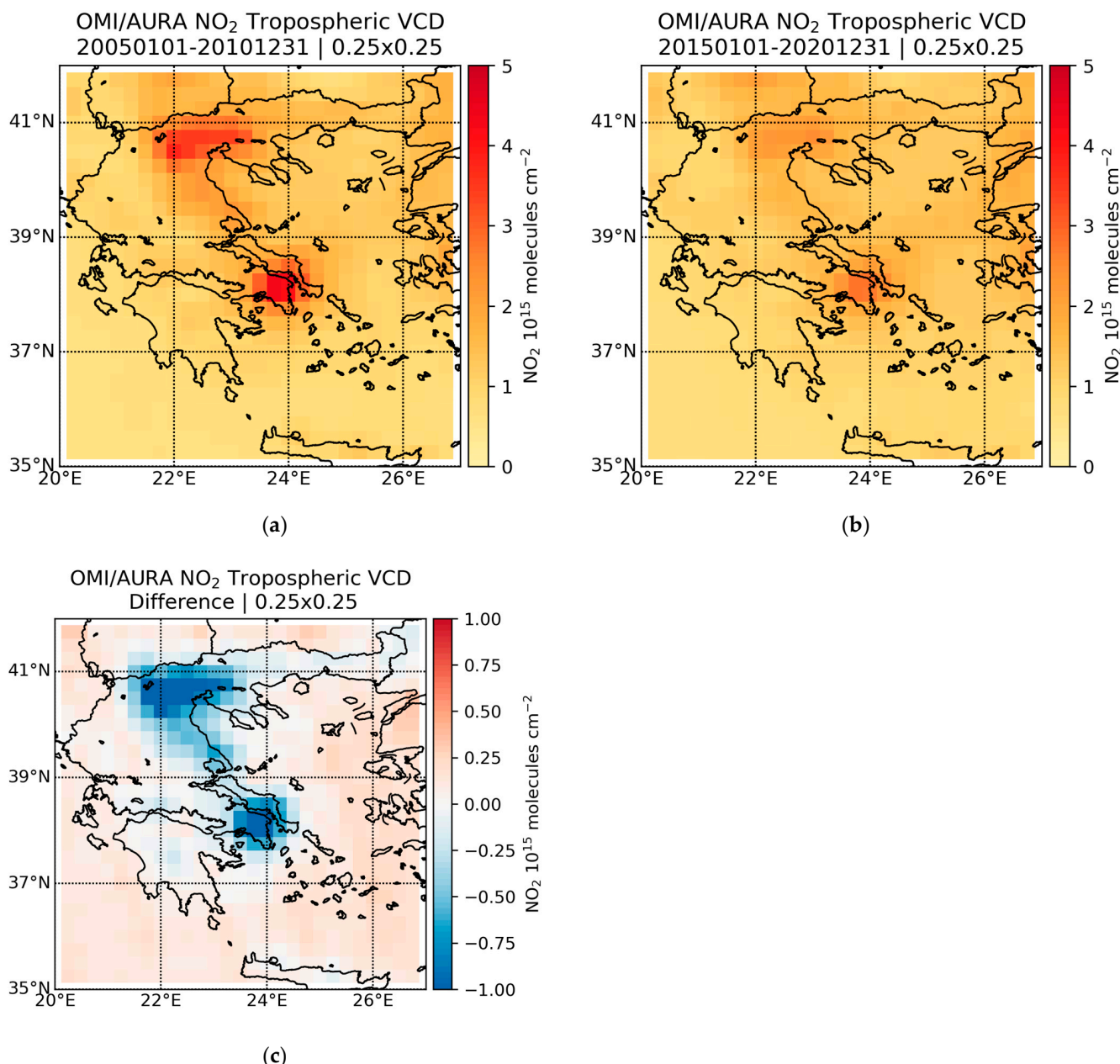


Figure 8. OMI/Aura observations over the Eastern Mediterranean. Mean tropospheric NO₂ vertical column densities [10^{15} molecules cm^{-2}] for 2005–2010 (a), 2015–2020 (b) and their difference (c). Data acquired from ([198]).

In Figure 9, we report the improvement in air quality over Greece, as observed by the OMI/Aura sensor tropospheric SO₂ levels for recent years. In the upper-right panel, the mean 2005–2010 tropospheric SO₂ vertical column densities show the high levels over the Megalopolis Power plant, to the south, as well as the Ptolemaida power plant in the northwest of the country. In the middle, based on the mean 2015–2020 levels, a marked decrease is reported for all high-emitting locations. In the lower panel, the absolute difference plot between the multi-annual means of 2005–2010 and 2015–2020 further demonstrates the decline in SO₂ emissions in recent times.

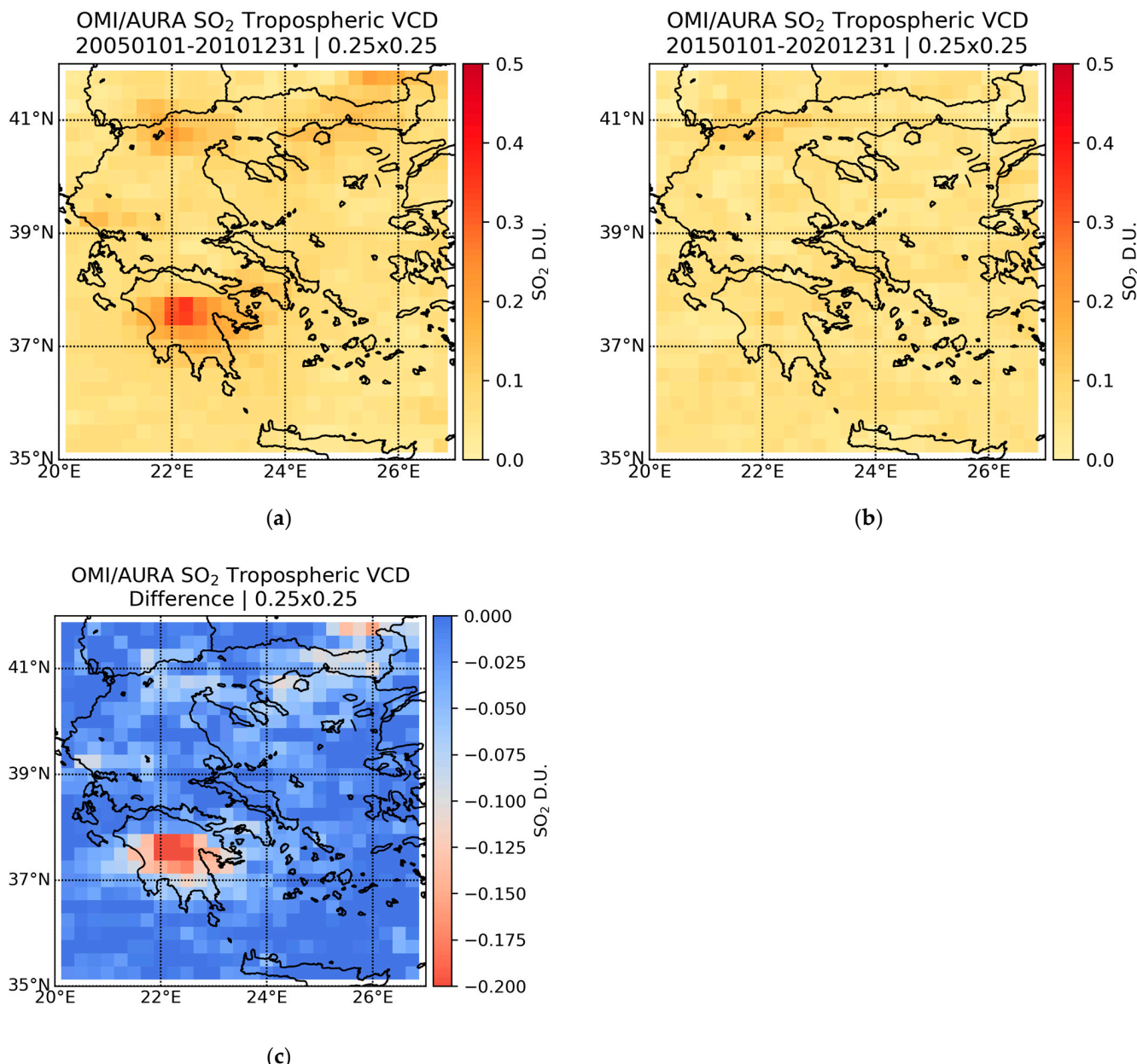


Figure 9. OMI/Aura observations over the Eastern Mediterranean. Mean tropospheric SO₂ vertical column densities [Dobson Units] for 2005–2010 (a), 2015–2020 (b) and their difference (c). Data acquired from ([198]).

2. Impacts

The regional climatic impacts of SLCFs mainly include the effects on solar radiation, temperature, visibility and biogeochemistry. SLCFs affect weather by affecting cloud formation and the energy balance. They also adversely affect air quality, human health and energy fields, while their deposition affects agricultural yield, ecosystem vitality and ocean productivity.

2.1. Solar Radiation

Shortwave radiation: In recent decades, surface solar radiation (SSR) and its transmission through the atmosphere have been of increasing interest due to the related impacts on climate. Long-term solar radiation measurements in Greece have been presented mainly in studies performed for Athens [211] and Thessaloniki [212,213]. For the city of Athens,

a long-term SSR record (1954 to 2012) and retrievals (1900–1953) from sunshine duration (SDU) showed a dimming period in 1955–1980, ($-2\% \text{ decade}^{-1}$) that matches various European long-term SSR-measurement-related studies. In addition, a brightening period in 1980–2012 ($+1.5\% \text{ decade}^{-1}$), both in the lower limit of the reported positive changes in SSR around Europe (Figure 10), was found. Such changes were linked mostly with aerosol changes. Considering Thessaloniki, for the period 1993 to 2011, a positive ($+3.3\% \text{ decade}^{-1}$) change was found. For the latest period, both studies refer to aerosol negative changes as a major factor for these SSR changes. More recent results [214] for 30 years of pyranometer data under three types of sky conditions (clear, cloudy and all sky) showed positive trends of $0.38\%/\text{year}$ for all sky, $\sim 0.1\%/\text{year}$ for clear sky and $0.41\%/\text{year}$ for cloudy conditions. Satellite and model-based results [215,216] revealed an increase in SSR (positive trends ranging from 0.1 to $5.2 \text{ W/m}^2/\text{decade}$), mostly related to a decrease in the aerosol optical depth and the liquid cloud fraction [209]. The analysis of long-term observations of SDU in 15 sites deployed across Greece showed that almost all sites have undergone a decrease in the annual SDU from 1960s until the mid-1980s [217]. In Athens, the annual SDU decreased by approximately 7% from the 1950s to 1980s and increased by 3% thereafter under all-sky conditions. Under clear-sky conditions, the increase in SDU after the 1980s is larger, amounting to 9% [218].

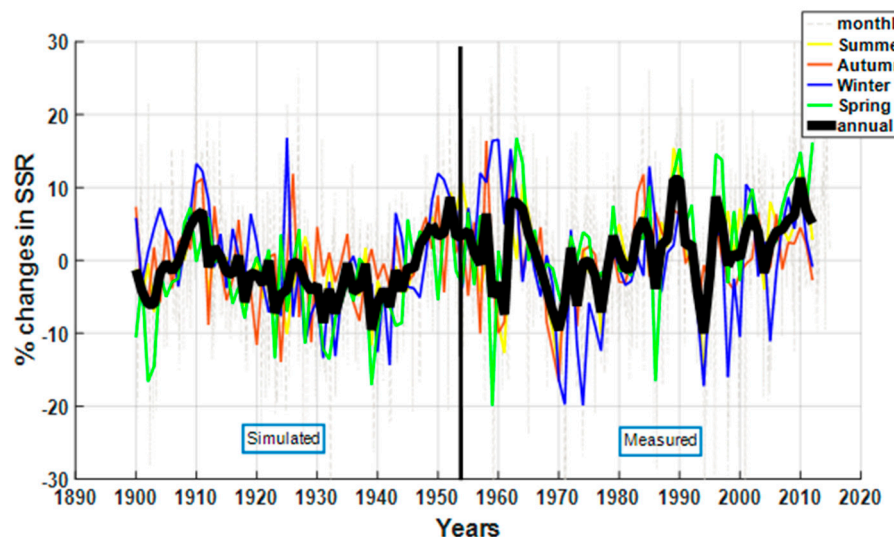


Figure 10. Long-term solar radiation changes in the city of Athens (source: [211]).

Solar UV: Despite the positive total ozone trends recorded in the last three decades and the expected recovery by the mid-2060s, additional uncertainties in solar UV are revealed due to clouds and aerosols, whose spatiotemporal variability depends on man-made climate change [219]. Over regions that are strongly affected by aerosols, such as the countries lying on the shores of the Mediterranean Sea, aerosols are among the main factors controlling the levels of surface solar UV radiation (e.g., [36,173,220–228]). Under intense aerosol events (e.g., wildfire smoke or combined smoke-dust events), aerosols can attenuate solar UV radiation at shorter wavelengths by more than 50% [75]. Analysis of the long, high-quality series of spectroradiometric UV measurements that are available in Thessaloniki, Greece [72,74,176,229–231], showed a significant reduction in AOD at UV wavelengths between 1997 and 2019 (of ~ 0.25 for the AOD at 320 nm for the whole period), with the reduction being stronger in the first half of the period [65,74]. The detected positive trends in UV radiation were related both to AOD and single scattering albedo changes, not only over Thessaloniki [71,73,74] but also in Athens, Greece [67,78,232]. Aerosols play a significant role in satellite-based UV retrieval algorithms [71,230–236]. Finally, the UV index Observation System (UVIOS) [237–240] was developed recently for UV index forecasting in Europe.

Solar Energy: Over relatively arid regions, the attenuation of solar radiation due to aerosols can be comparable or even more significant relative to the attenuation by clouds (e.g., [241–246]). Papachristopoulou et al. [26] estimated that over the broader Mediterranean basin, the average attenuation of annual global horizontal irradiation (GHI) and direct normal irradiation (DNI) by aerosols for 2003–2017 was 1–13% and 5–47%, respectively, with the dust component having a very significant contribution (up to 90% over North Africa and the Middle East). Fountoulakis et al. [25] estimated that in Cyprus, aerosols attenuate 5–10% of the annual GHI and 15–35% of the annual DNI, with dust being responsible for 30–50% of the overall attenuation. Nikitidou et al. [247] and Kosmopoulos et al. [248] reported a very high GHI reduction due to dust during an extreme event over the Eastern Mediterranean. Kouklaki et al. [249] showed that the effects of smoke and dust aerosols on the solar energy production vary, while, in general, smoke has a more significant effect than dust. The significant role of aerosols in the production of solar energy in Greece was also highlighted in studies by Kambezidis [250] and Kazantzidis et al. [243]. Nikitidou et al. [251] and Zempila et al. [252] evaluated satellite-derived irradiance and four shortwave radiation schemes of the mesoscale atmospheric Weather Research and Forecasting (WRF) model in terms of GHI using measurements at 12 stations of the Hellenic Network of Solar Energy [253]. The Hellenic Network of Solar Energy initially comprised 12 stations, with the location of each station determined from cluster analysis of satellite-derived cloud estimations [254]. Artificial neural networks (ANNs) were trained according to that cluster analysis to improve estimations of GHI and DNI [255]. An effort to further understand how different types of clouds affect GHI has been made [256]. For the optimization of energy production, the effects of clouds and aerosols must be considered for the installation of photovoltaics [257,258]. Finally, a solar energy nowcasting and short-term forecasting (3 h ahead) system (nextSENSE) was recently developed [259–261] to simulate surface solar irradiance, with a high spatial (5 km) and temporal (15 min) resolution for Europe. Validation of the model estimates [262] and forecasts [263] showed that uncertainties in the simulated quantities over Greek sites are mainly due to the parameterization of cloudiness, while aerosols have a more significant impact on the DNI relative to the GHI.

2.2. Visibility

Atmospheric visibility is defined as the greatest distance at which a black object of suitable dimensions can be seen and recognized in daylight [264] and is a strong indicator of air quality in an area. Greece, located in the Eastern Mediterranean, experiences humid air mass transport from over the Mediterranean basin, episodically high dust loads from N. Africa and the impact of anthropogenic (cities) pollution [31]. Founda et al. [217] reported a striking decrease in visibility in Athens since the early 1930s, attributed to regional and local air pollution, related to high urbanization and regional emission rates after the 1950s. Visibility in Athens was highly determined by wind direction and corresponding origin of the air mass, PM10 and AOD. Cloudiness measurements in the Athens area have existed since 1882 based on observations at the National Observatory of Athens historical Thissio station. Founda et al. [265] reported statistically significant positive trends in cloud cover, more pronounced in spring and summer.

2.3. Biogeochemistry

Atmospheric transport may drastically change aerosols' key properties and consequently affect marine and terrestrial ecosystems following the particles' atmospheric deposition. Acid processing of atmospheric dust aerosols affects the solubility of trace metals, like Fe- and P-containing aerosols, which can then become readily available to ecosystems [266–268]. Given the high concentration of both pollutants and mineral dust in the Mediterranean, their interactions are critical for understanding the broader impacts of human activities on ecosystems and climate throughout the Mediterranean area. Emissions from biomass burning and anthropogenic combustion also contribute to the soluble

Fe [269,270], P [271,272] and N [273] levels and can impact marine biogeochemistry through the atmospheric deposition pathway [270,274].

Myriokefalitakis et al. [275] calculated an increase since preindustrial times in submicron aerosol acidity from the anthropogenic and biomass-burning emissions in the region, while a reduction is projected in the future due to the mitigation of air pollution. Kanakidou et al. [276] calculated enhanced mineral Fe and P dissolution fluxes over the Eastern Mediterranean basin and the Middle East. Nenes et al. [277] also proposed that the processing of mineral aerosol under acidic conditions may increase the bioavailability of phosphorus in soil dust in the presence of atmospheric pollutants. Overall, model simulations undoubtedly indicate that acid-promoted dust dissolution impacts nutrient inputs into the Mediterranean Sea by increasing the soluble Fe and P deposition fluxes [278]. The significant contribution of natural sources to the particulate matter of the region combined with high background regional air pollutant levels, especially in the southeast of the Mediterranean basin, is, nevertheless, shown to be critical for the Mediterranean marine ecosystem and particularly the primary productivity in the region, possibly accounting for up to half of the net primary production rates (see [276]). Recent work by Violaki et al. [278] showed that Saharan dust is an important primary source of bioavailable P to the Eastern Mediterranean, especially during the spring period, when 60% of the events occurred. However, the heterogeneity in acidic and alkaline emissions may non-linearly impact the dust acidification and the produced nutrients transferred into the Mediterranean Sea.

3. Summary and Recommendations

The Eastern Mediterranean experiences high aerosol concentrations of both a natural and anthropogenic origin, with high spatiotemporal variability. Natural aerosols (desert dust, fire smoke, sea salt and volcanic ash) have been fluctuating over time with different rates, and these fluctuations are linked with certain seasons and patterns possibly affected by climate change (meteorological, geographical, climatic). Aerosol effects include a number of aspects related to the regional weather and climate, solar radiation, visibility, health and aviation.

Up to now, the monitoring of aerosols and their precursors in Greece has been valuable for the identification of aerosol types and sources, their origin and their effects on tropospheric chemistry, visibility, health, solar radiation and energy. Nevertheless, a consolidated analysis of the SLCF trends over Greece based on the synergy of observations is currently incomplete and sporadic, mainly due to the limited coverage of the ground-based monitoring stations and the lack of synergistic studies using ground-based and satellite observations. As such, a comprehensive analysis of a multi-sensor record of observations is recommended. Moreover, an assessment of the factors driving the aerosol burden's temporal variability would be essential. Such a challenging and demanding task can be addressed via the integration of diverse information sources (i.e., observations, modelling, re-analyses) describing environmental processes, which act across various spatiotemporal scales. The outcomes of such analyses will aid the climate modelling community in upgrading the representation of key mechanisms in the numerical simulations and constraining the related uncertainties. This, in turn, will enhance the reliability of SLCF future projections and the associated induced impacts on climate, and vice versa, in the forthcoming decades.

Aerosol typing studies from the synergy of observations and models would also be beneficial for decomposing the role of different sources to specific impacts and sectors. Ground-based European and global observational networks (AERONET, EARLINET, Pandonia, BSRN, WMO-GAW) and research infrastructures (ACTRIS, ICOS, PANACEA) are essential for the continuation of the climate data records in Greece. This is especially important due to the existence of unique and scientifically significant historic data records of crucial parameters, such as AOD, total ozone, solar irradiance, aerosol profiles, sunshine duration, visibility, cloudiness and others, maintained and processed by different research groups in Greece. For the continuation of such measurements, national and European funding related to research infrastructures, space-borne remote sensing and related science

projects are imperative. In addition, a denser network of stations would be beneficial for improving the spatiotemporal representation of SLFCs and for enhancing satellite calibration and validation (Cal/Val) activities in the region.

The challenges for reducing the aerosol uncertainties through the enhancement of our knowledge can be summarized as follows:

1. Enhancing and upgrading ground-based monitoring infrastructures through global and European network initiatives, driven by a significant national mandate;
2. Obtaining systematic aircraft and UAV in situ measurements of aerosol microphysical and chemical properties combined with meteorology for the major aerosol types and air masses, to facilitate closure studies that will enhance our knowledge on aerosol variability and concomitant effects;
3. Focusing on research for integrating satellite observations, suborbital measurements and modeling (including data assimilation).

Major aspects to be addressed concern the coherent and continuous monitoring of SLFCs in Greece, aerosol typing and separation of anthropogenic and natural aerosols, aerosol load temporal variability, aerosol model downscaling aspects, aerosol–cloud–radiation interactions, solar energy high-spatiotemporal-resolution forecasting and satellite validation activities in the diverse aerosol-wise Greek environment.

Author Contributions: Conceptualization, V.A. and S.K.; methodology, A.G. (Antonis Gkikas), M.-E.K., K.G. and A.K.G.; formal analysis, K.A.V., D.K., A.K. (Anna Kampouri) and K.P.; investigation, D.F., B.E.P., P.K. (Petros Katsafados), P.K. (Pavlos Kalabokas) and I.F.; data curation, P.-I.R., A.G. (Antonis Gkikas), S.S., E.P., G.V., A.T., E.D., E.M., E.G., S.M., J.K. and T.G.; writing—review and editing, K.E., V.A., S.K., A.G. (Anna Gialitaki), M.-E.K., N.H., A.G. (Antonis Gkikas), P.K. (Petros Katsafados), P.K. (Pavlos Kalabokas), P.Z., M.V., A.P., A.K. (Andreas Kazantzidis), K.K., D.B., A.F.B. and C.Z. All authors have read and agreed to the published version of the manuscript.

Funding: This research was funded by the Hellenic Foundation for Research and Innovation (H.F.R.I.) under the “3rd Call for H.F.R.I. Research Projects to support Post-Doctoral Researchers” (Project Acronym: REVEAL, Project Number: 07222). V. A. acknowledges support by the projects: “Support for Enhancing the Operation of the National Network for Climate Change (CLIMPACT)”, National Development Program, General Secretariat of Research and Innovation, Greece (2023NA11900001—N. 5201588); the Harmonia Action (no. CA21119) supported by COST (European Cooperation in Science and Technology); the Horizon Europe programme under Grant Agreement No 101137680 via project CERTAINTY (Cloud-aERosol inTeractions & their impActS IN The earth sYstem); the AIRSENSE which is a part of Atmosphere Science Cluster of ESA’s EO Science for Society programme, and the Hellenic Foundation for Research and Innovation (Project Acronym: StratoFIRE, Project Number: 3995). E. P. acknowledges support by the AXA Research Fund for postdoctoral researchers under the project entitled “Earth Observation for Air-Quality—Dust Fine-Mode (EO4AQ-DustFM). KAV acknowledges support by the PANGEA4CalVal (grant agreement no. 101079201) funded by the European Union. A. Gkikas acknowledges support by the Hellenic Foundation for Research and Innovation (H.F.R.I.) under the “2nd Call for H.F.R.I. Research Projects to support Post-Doctoral Researchers” (Project Number: 544).

Acknowledgments: This research was supported by data and services obtained from the ACTRIS Research Infrastructure and the PANhellenic Geophysical Observatory of Antikythera (PANGEA) of the National Observatory of Athens (NOA).

Conflicts of Interest: The authors declare no conflicts of interest.

References

1. Szopa, S.; Naik, V.; Adhikary, B.; Artaxo, P.; Berntsen, T.; Collins, W.D.; Fuzzi, S.; Gallardo, L.; Kiendler-Scharr, A.; Klimont, Z.; et al. Short-Lived Climate Forcers. In *Climate Change 2021: The Physical Science Basis. Contribution of Working Group I to the Sixth Assessment Report of the Intergovernmental Panel on Climate Change*; Masson-Delmotte, V., Zhai, P., Pirani, A., Connors, S.L., Péan, C., Berger, S., Caud, N., Chen, Y., Goldfarb, L., Gomis, M.I., et al., Eds.; Cambridge University Press: Cambridge, UK; New York, NY, USA, 2021; pp. 817–922. [[CrossRef](#)]

2. Lelieveld, J.; Hadjinicolaou, P.; Kostopoulou, E.; Chenoweth, J.; El Maayar, M.; Giannakopoulos, C.; Hannides, C.; Lange, M.A.; Tanarhte, M.; Tyrlis, E.; et al. Climate change and impacts in the Eastern Mediterranean and the Middle East. *Clim. Chang.* **2012**, *114*, 667–687. [[CrossRef](#)] [[PubMed](#)]
3. Moulin, C.; Lambert, C.E.; Dayan, U.; Masson, V.; Ramonet, M.; Bousquet, P.; Legrand, M.; Balkanski, Y.J.; Guelle, W.; Marticorena, B.; et al. Satellite climatology of African dust transport in the Mediterranean atmosphere. *J. Geophys. Res. Atmos.* **1998**, *103*, 13137–13144. [[CrossRef](#)]
4. Nabat, P.; Somot, S.; Mallet, M.; Chiapello, I.; Morcrette, J.J.; Solmon, F.; Szopa, S.; Dulac, F.; Collins, W.; Ghan, S.; et al. A 4-D climatology (1979–2009) of the monthly tropospheric aerosol optical depth distribution over the Mediterranean region from a comparative evaluation and blending of remote sensing and model products. *Atmos. Meas. Tech.* **2013**, *6*, 1287–1314. [[CrossRef](#)]
5. Koukouli, M.E.; Balis, D.S.; Amiridis, V.; Kazadzis, S.; Bais, A.; Nickovic, S.; Torres, O. Aerosol variability over Thessaloniki using ground based remote sensing observations and the TOMS aerosol index. *Atmos. Environ.* **2006**, *40*, 5367–5378. [[CrossRef](#)]
6. Koukouli, M.E.; Kazadzis, S.; Amiridis, V.; Ichoku, C.; Balis, D.S.; Bais, A.F. Signs of a negative trend in the MODIS aerosol optical depth over the Southern Balkans. *Atmos. Environ.* **2010**, *44*, 1219–1228. [[CrossRef](#)]
7. Hatzianastassiou, N.; Gkikas, A.; Mihalopoulos, N.; Torres, O.; Katsoulis, B.D. Natural versus anthropogenic aerosols in the eastern Mediterranean basin derived from multiyear TOMS and MODIS satellite data. *J. Geophys. Res. Atmos.* **2009**, *114*, 2009JD011982. [[CrossRef](#)]
8. Gkikas, A.; Hatzianastassiou, N.; Mihalopoulos, N.; Katsoulis, V.; Kazadzis, S.; Pey, J.; Querol, X.; Torres, O. The regime of intense desert dust episodes in the Mediterranean based on contemporary satellite observations and ground measurements. *Atmos. Chem. Phys.* **2013**, *13*, 12135–12154. [[CrossRef](#)]
9. Gkikas, A.; Houssos, E.E.; Lolis, C.J.; Bartzokas, A.; Mihalopoulos, N.; Hatzianastassiou, N. Atmospheric circulation evolution related to desert-dust episodes over the Mediterranean. *Q. J. R. Meteorol. Soc.* **2015**, *141*, 1634–1645. [[CrossRef](#)]
10. Kaskaoutis, D.G.; Gautam, R.; Singh, R.P.; Houssos, E.E.; Goto, D.; Singh, S.; Bartzokas, A.; Kosmopoulos, P.G.; Sharma, M.; Hsu, N.C.; et al. Influence of anomalous dry conditions on aerosols over India: Transport, distribution and properties. *J. Geophys. Res. Atmos.* **2012**, *117*, D09106. [[CrossRef](#)]
11. Kosmopoulos, P.G.; Kaskaoutis, D.G.; Nastos, P.T.; Kambezidis, H.D. Seasonal variation of columnar aerosol optical properties over Athens, Greece, based on MODIS data. *Remote Sens. Environ.* **2008**, *112*, 2354–2366. [[CrossRef](#)]
12. Papadimas, C.D.; Hatzianastassiou, N.; Mihalopoulos, N.; Querol, X.; Vardavas, I. Spatial and temporal variability in aerosol properties over the Mediterranean basin based on 6-year (2000–2006) MODIS data. *J. Geophys. Res. Atmos.* **2008**, *113*, D11205. [[CrossRef](#)]
13. Papadimas, C.D.; Hatzianastassiou, N.; Mihalopoulos, N.; Kanakidou, M.; Katsoulis, B.D.; Vardavas, I. Assessment of the MODIS Collections C005 and C004 aerosol optical depth products over the Mediterranean basin. *Atmos. Chem. Phys.* **2009**, *9*, 2987–2999. [[CrossRef](#)]
14. Gkikas, A.; Hatzianastassiou, N.; Mihalopoulos, N. Aerosol events in the broader Mediterranean basin based on 7-year (2000–2007) MODIS C005 data. *Ann. Geophys.* **2009**, *27*, 3509–3522. [[CrossRef](#)]
15. Gkikas, A.; Proestakis, E.; Amiridis, V.; Kazadzis, S.; Di Tomaso, E.; Tsekeri, A.; Marinou, E.; Hatzianastassiou, N.; Pérez García-Pando, C. ModIs Dust AeroSol (MIDAS): A global fine-resolution dust optical depth data set. *Atmos. Meas. Tech.* **2021**, *14*, 309–334. [[CrossRef](#)]
16. Gkikas, A.; Proestakis, E.; Amiridis, V.; Kazadzis, S.; Di Tomaso, E.; Marinou, E.; Hatzianastassiou, N.; Kok, J.F.; García-Pando, C.P. Quantification of the dust optical depth across spatiotemporal scales with the MIDAS global dataset (2003–2017). *Atmos. Chem. Phys.* **2022**, *22*, 3553–3578. [[CrossRef](#)]
17. Nikitidou, E.; Kazantzidis, A. On the differences of ultraviolet and visible irradiance calculations in the Mediterranean basin due to model- and satellite-derived climatologies of aerosol optical properties. *Int. J. Climatol.* **2013**, *33*, 2877–2888. [[CrossRef](#)]
18. Athanassiou, G.; Hatzianastassiou, N.; Gkikas, A.; Papadimas, C.D. Estimating Aerosol Optical Depth Over the Broader Greek Area from MODIS Satellite. *Water Air Soil. Pollut.* **2013**, *224*, 1605. [[CrossRef](#)]
19. Benas, N.; Beloconi, A.; Chrysoulakis, N. Estimation of urban PM10 concentration, based on MODIS and MERIS/AATSR synergistic observations. *Atmos. Environ.* **2013**, *79*, 448–454. [[CrossRef](#)]
20. Kourtidis, K.; Rapsomanikis, S.; Zerefos, C.; Georgoulias, A.K.; Pavlidou, E. Severe particulate pollution from the deposition practices of the primary materials of a cement plant. *Environ. Sci. Pollut. Res.* **2014**, *21*, 9796–9808. [[CrossRef](#)]
21. Flaounas, E.; Kotroni, V.; Lagouvardos, K.; Kazadzis, S.; Gkikas, A.; Hatzianastassiou, N. Cyclone contribution to dust transport over the Mediterranean region. *Atmos. Sci. Lett.* **2015**, *16*, 473–478. [[CrossRef](#)]
22. Georgoulias, A.K.; Alexandri, G.; Kourtidis, K.A.; Lelieveld, J.; Zanis, P.; Pöschl, U.; Levy, R.; Amiridis, V.; Marinou, E.; Tsikerdekis, A. Spatiotemporal variability and contribution of different aerosol types to the aerosol optical depth over the Eastern Mediterranean. *Atmos. Chem. Phys.* **2016**, *16*, 13853–13884. [[CrossRef](#)] [[PubMed](#)]
23. Georgoulias, A.K.; Alexandri, G.; Kourtidis, K.A.; Lelieveld, J.; Zanis, P.; Amiridis, V. Differences between the MODIS Collection 6 and 5.1 aerosol datasets over the greater Mediterranean region. *Atmos. Environ.* **2016**, *147*, 310–319. [[CrossRef](#)]
24. Logothetis, S.-A.; Salamalikis, V.; Gkikas, A.; Kazadzis, S.; Amiridis, V.; Kazantzidis, A. 15-year variability of desert dust optical depth on global and regional scales. *Atmos. Chem. Phys.* **2021**, *21*, 16499–16529. [[CrossRef](#)]

25. Fountoulakis, I.; Kosmopoulos, P.; Papachristopoulou, K.; Raptis, I.-P.; Mamouri, R.-E.; Nisantzi, A.; Gkikas, A.; Withuhn, J.; Bley, S.; Moustaka, A.; et al. Effects of Aerosols and Clouds on the Levels of Surface Solar Radiation and Solar Energy in Cyprus. *Remote Sens.* **2021**, *13*, 2319. [[CrossRef](#)]
26. Papachristopoulou, K.; Fountoulakis, I.; Gkikas, A.; Kosmopoulos, P.G.; Nastos, P.T.; Hatzaki, M.; Kazadzis, S. 15-Year Analysis of Direct Effects of Total and Dust Aerosols in Solar Radiation/Energy over the Mediterranean Basin. *Remote Sens.* **2022**, *14*, 1535. [[CrossRef](#)]
27. Kaskaoutis, D.G.; Nastos, P.T.; Kosmopoulos, P.G.; Kambezidis, H.D. The combined use of satellite data, air-mass trajectories and model applications for monitoring dust transport over Athens, Greece. *Int. J. Remote Sens.* **2010**, *31*, 5089–5109. [[CrossRef](#)]
28. Amiridis, V.; Kafatos, M.; Perez, C.; Kazadzis, S.; Gerasopoulos, E.; Mamouri, R.E.; Papayannis, A.; Kokkalis, P.; Giannakaki, E.; Basart, S.; et al. The potential of the synergistic use of passive and active remote sensing measurements for the validation of a regional dust model. *Ann. Geophys.* **2009**, *27*, 3155–3164. [[CrossRef](#)]
29. Amiridis, V.; Wandinger, U.; Marinou, E.; Giannakaki, E.; Tsekeri, A.; Basart, S.; Kazadzis, S.; Gkikas, A.; Taylor, M.; Baldasano, J.; et al. Optimizing CALIPSO Saharan dust retrievals. *Atmos. Chem. Phys.* **2013**, *13*, 12089–12106. [[CrossRef](#)]
30. Marinou, E.; Amiridis, V.; Binietoglou, I.; Tsikerdekkis, A.; Solomos, S.; Proestakis, E.; Konsta, D.; Papagiannopoulos, N.; Tsekeri, A.; Vlastou, G.; et al. Three-dimensional evolution of Saharan dust transport towards Europe based on a 9-year EARLINET-optimized CALIPSO dataset. *Atmos. Chem. Phys.* **2017**, *17*, 5893–5919. [[CrossRef](#)]
31. Kanakidou, M.; Mihalopoulos, N.; Kindap, T.; Im, U.; Vrekoussis, M.; Gerasopoulos, E.; Dermitzaki, E.; Unal, A.; Koçak, M.; Markakis, K.; et al. Megacities as hot spots of air pollution in the East Mediterranean. *Atmos. Environ.* **2011**, *45*, 1223–1235. [[CrossRef](#)]
32. Retalis, A.; Sifakis, N. Urban aerosol mapping over Athens using the differential textural analysis (DTA) algorithm on MERIS-ENVISAT data. *ISPRS J. Photogramm. Remote Sens.* **2010**, *65*, 17–25. [[CrossRef](#)]
33. Sifakis, N.I.; Iossifidis, C.; Kontoes, C. CHRISTINE Code for High Resolution Satellite mapping of optical Thickness and Ångstrom Exponent. Part II: First application to the urban area of Athens, Greece and comparison to results from previous contrast-reduction codes. *Comput. Geosci.* **2014**, *62*, 142–149. [[CrossRef](#)]
34. Papayannis, A.; Balis, D. Study of the structure of the lower troposphere over Athens using a backscattering lidar during the MEDCAPOT-TRACE experiment. *Atmos. Environ.* **1998**, *32*, 2161–2172. [[CrossRef](#)]
35. Balis, D.S.; Amiridis, V.; Nickovic, S.; Papayannis, A.; Zerefos, C. Optical properties of Saharan dust layers as detected by a Raman lidar at Thessaloniki, Greece. *Geophys. Res. Lett.* **2004**, *31*, 2004GL019881. [[CrossRef](#)]
36. Balis, D.S.; Amiridis, V.; Zerefos, C.; Kazantzidis, A.; Kazadzis, S.; Bais, A.F.; Meleti, C.; Gerasopoulos, E.; Papayannis, A.; Matthias, V.; et al. Study of the effect of different type of aerosols on UV-B radiation from measurements during EARLINET. *Atmos. Chem. Phys.* **2004**, *4*, 307–321. [[CrossRef](#)]
37. Balis, D.; Amiridis, V.; Kazadzis, S.; Papayannis, A.; Tsaknakis, G.; Tzortzakis, S.; Kalivitis, N.; Vrekoussis, M.; Kanakidou, M.; Mihalopoulos, N.; et al. Optical characteristics of desert dust over the East Mediterranean during summer: A case study. *Ann. Geophys.* **2006**, *24*, 807–821. [[CrossRef](#)]
38. Papayannis, A.; Chourdakis, G. The EOLE Project: A multiwavelength laser remote sensing (lidar) system for ozone and aerosol measurements in the troposphere and the lower stratosphere. Part II: Aerosol measurements over Athens, Greece. *Int. J. Remote Sens.* **2002**, *23*, 179–196. [[CrossRef](#)]
39. Papayannis, A.; Balis, D.; Amiridis, V.; Chourdakis, G.; Tsaknakis, G.; Zerefos, C.; Castanho, A.D.A.; Nickovic, S.; Kazadzis, S.; Grabowski, J. Measurements of Saharan dust aerosols over the Eastern Mediterranean using elastic backscatter-Raman lidar, spectrophotometric and satellite observations in the frame of the EARLINET project. *Atmos. Chem. Phys.* **2005**, *5*, 2065–2079. [[CrossRef](#)]
40. Papayannis, A.; Amiridis, V.; Mona, L.; Tsaknakis, G.; Balis, D.; Bösenberg, J.; Chaikovski, A.; De Tomasi, F.; Grigorov, I.; Mattis, I.; et al. Systematic lidar observations of Saharan dust over Europe in the frame of EARLINET (2000–2002). *J. Geophys. Res. Atmos.* **2008**, *113*, D10204. [[CrossRef](#)]
41. Papayannis, A.; Mamouri, R.E.; Amiridis, V.; Kazadzis, S.; Pérez, C.; Tsaknakis, G.; Kokkalis, P.; Baldasano, J.M. Systematic lidar observations of Saharan dust layers over Athens, Greece in the frame of EARLINET project (2004–2006). *Ann. Geophys.* **2009**, *27*, 3611–3620. [[CrossRef](#)]
42. Papayannis, A.; Mamouri, R.E.; Amiridis, V.; Giannakaki, E.; Veselovskii, I.; Kokkalis, P.; Tsaknakis, G.; Balis, D.; Kristiansen, N.I.; Stohl, A.; et al. Optical properties and vertical extension of aged ash layers over the Eastern Mediterranean as observed by Raman lidars during the Eyjafjallajökull eruption in May 2010. *Atmos. Environ.* **2012**, *48*, 56–65. [[CrossRef](#)]
43. Amiridis, V.; Balis, D.S.; Kazadzis, S.; Bais, A.; Giannakaki, E.; Papayannis, A.; Zerefos, C. Four-year aerosol observations with a Raman lidar at Thessaloniki, Greece, in the framework of European Aerosol Research Lidar Network (EARLINET). *J. Geophys. Res. Atmos.* **2005**, *110*, D21203. [[CrossRef](#)]
44. Amiridis, V.; Balis, D.S.; Giannakaki, E.; Stohl, A.; Kazadzis, S.; Koukouli, M.E.; Zanis, P. Optical characteristics of biomass burning aerosols over Southeastern Europe determined from UV-Raman lidar measurements. *Atmos. Chem. Phys.* **2009**, *9*, 2431–2440. [[CrossRef](#)]
45. Giannakaki, E.; Balis, D.S.; Amiridis, V.; Zerefos, C. Optical properties of different aerosol types: Seven years of combined Raman-elastic backscatter lidar measurements in Thessaloniki, Greece. *Atmos. Meas. Tech.* **2010**, *3*, 569–578. [[CrossRef](#)]

46. Mamouri, R.E.; Papayannis, A.; Amiridis, V.; Müller, D.; Kokkalis, P.; Rapsomanikis, S.; Karageorgos, E.T.; Tsaknakis, G.; Nenes, A.; Kazadzis, S.; et al. Multi-wavelength Raman lidar, sun photometric and aircraft measurements in combination with inversion models for the estimation of the aerosol optical and physico-chemical properties over Athens, Greece. *Atmos. Meas. Tech.* **2012**, *5*, 1793–1808. [[CrossRef](#)]
47. Kokkalis, P.; Papayannis, A.; Amiridis, V.; Mamouri, R.E.; Veselovskii, I.; Kolgotin, A.; Tsaknakis, G.; Kristiansen, N.I.; Stohl, A.; Mona, L. Optical, microphysical, mass and geometrical properties of aged volcanic particles observed over Athens, Greece, during the Eyjafjallajökull eruption in April 2010 through synergy of Raman lidar and sunphotometer measurements. *Atmos. Chem. Phys.* **2013**, *13*, 9303–9320. [[CrossRef](#)]
48. Siomos, N.; Balis, D.S.; Voudouri, K.A.; Giannakaki, E.; Filioglou, M.; Amiridis, V.; Papayannis, A.; Frangkos, K. Are EARLINET and AERONET climatologies consistent? The case of Thessaloniki, Greece. *Atmos. Chem. Phys.* **2018**, *18*, 11885–11903. [[CrossRef](#)]
49. Soupliou, O.; Papayannis, A.; Kokkalis, P.; Mylonaki, M.; Tsaknakis, G.; Argyrouli, A.; Vratolis, S. Long-term systematic profiling of dust aerosol optical properties using the EOLE NTUA lidar system over Athens, Greece (2000–2016). *Atmos. Environ.* **2018**, *183*, 165–174. [[CrossRef](#)]
50. Soupliou, O.; Samaras, S.; Ortiz-Amezcua, P.; Böckmann, C.; Papayannis, A.; Moreira, G.A.; Benavent-Oltra, J.A.; Guerrero-Rascado, J.L.; Bedoya-Velásquez, A.E.; Olmo, F.J.; et al. Retrieval of optical and microphysical properties of transported Saharan dust over Athens and Granada based on multi-wavelength Raman lidar measurements: Study of the mixing processes. *Atmos. Environ.* **2019**, *214*, 116824. [[CrossRef](#)]
51. Voudouri, K.A.; Siomos, N.; Michailidis, K.; Papagiannopoulos, N.; Mona, L.; Cornacchia, C.; Nicolae, D.; Balis, D. Comparison of two automated aerosol typing methods and their application to an EARLINET station. *Atmos. Chem. Phys.* **2019**, *19*, 10961–10980. [[CrossRef](#)]
52. Voudouri, K.A.; Michailidis, K.; Siomos, N.; Chatzopoulou, A.; Kouvarakis, G.; Mihalopoulos, N.; Tzoumaka, P.; Kelessis, A.; Balis, D. Evaluation of Aerosol Typing with Combination of Remote Sensing Techniques with In Situ Data during the PANACEA Campaigns in Thessaloniki Station, Greece. *Remote Sens.* **2022**, *14*, 5076. [[CrossRef](#)]
53. Voudouri, K.A.; Michailidis, K.; Koukouli, M.-E.; Rémy, S.; Inness, A.; Taha, G.; Peletidou, G.; Siomos, N.; Balis, D.; Parrington, M. Investigating a Persistent Stratospheric Aerosol Layer Observed over Southern Europe during 2019. *Remote Sens.* **2023**, *15*, 5394. [[CrossRef](#)]
54. Gialitaki, A.; Tsekeli, A.; Amiridis, V.; Ceolato, R.; Paulien, L.; Kampouri, A.; Gkikas, A.; Solomos, S.; Marinou, E.; Haarig, M.; et al. Is the near-spherical shape the “new black” for smoke? *Atmos. Chem. Phys.* **2020**, *20*, 14005–14021. [[CrossRef](#)]
55. Mylonaki, M.; Giannakaki, E.; Papayannis, A.; Papanikolaou, C.-A.; Komppula, M.; Nicolae, D.; Papagiannopoulos, N.; Amodeo, A.; Baars, H.; Soupliou, O. Aerosol type classification analysis using EARLINET multiwavelength and depolarization lidar observations. *Atmos. Chem. Phys.* **2021**, *21*, 2211–2227. [[CrossRef](#)]
56. Mylonaki, M.; Papayannis, A.; Anagnou, D.; Veselovskii, I.; Papanikolaou, C.-A.; Kokkalis, P.; Soupliou, O.; Foskinis, R.; Gidarakou, M.; Kralli, E. Optical and Microphysical Properties of Aged Biomass Burning Aerosols and Mixtures, Based on 9-Year Multiwavelength Raman Lidar Observations in Athens, Greece. *Remote Sens.* **2021**, *13*, 3877. [[CrossRef](#)]
57. Drosoglou, T.; Bais, A.F.; Zyrichidou, I.; Kouremeti, N.; Poupkou, A.; Liora, N.; Giannaros, C.; Koukouli, M.E.; Balis, D.; Melas, D. Comparisons of ground-based tropospheric NO₂ MAX-DOAS measurements to satellite observations with the aid of an air quality model over the Thessaloniki area, Greece. *Atmos. Chem. Phys.* **2017**, *17*, 5829–5849. [[CrossRef](#)]
58. Gkertsis, F.; Bais, A.F.; Kouremeti, N.; Drosoglou, T.; Fountoulakis, I.; Fragkos, K. DOAS-based total column ozone retrieval from Phaethon system. *Atmos. Environ.* **2018**, *180*, 51–58. [[CrossRef](#)]
59. Gratsea, M.; Vrekoussis, M.; Richter, A.; Wittrock, F.; Schönhardt, A.; Burrows, J.; Kazadzis, S.; Mihalopoulos, N.; Gerasopoulos, E. Slant column MAX-DOAS measurements of nitrogen dioxide, formaldehyde, glyoxal and oxygen dimer in the urban environment of Athens. *Atmos. Environ.* **2016**, *135*, 118–131. [[CrossRef](#)]
60. Gratsea, M.; Bösch, T.; Kokkalis, P.; Richter, A.; Vrekoussis, M.; Kazadzis, S.; Tsekeli, A.; Papayannis, A.; Mylonaki, M.; Amiridis, V.; et al. Retrieval and evaluation of tropospheric-aerosol extinction profiles using multi-axis differential optical absorption spectroscopy (MAX-DOAS) measurements over Athens, Greece. *Atmos. Meas. Tech.* **2021**, *14*, 749–767. [[CrossRef](#)]
61. Gratsea, M.; Athanasopoulou, E.; Kakouri, A.; Richter, A.; Seyler, A.; Gerasopoulos, E. Five Years of Spatially Resolved Ground-Based MAX-DOAS Measurements of Nitrogen Dioxide in the Urban Area of Athens: Synergies with In Situ Measurements and Model Simulations. *Atmosphere* **2021**, *12*, 1634. [[CrossRef](#)]
62. Karagkiozidis, D.; Friedrich, M.M.; Beirle, S.; Bais, A.; Hendrick, F.; Voudouri, K.A.; Fountoulakis, I.; Karanikolas, A.; Tzoumaka, P.; Van Roozendael, M.; et al. Retrieval of tropospheric aerosol, NO₂ and HCHO vertical profiles from MAX-DOAS observations over Thessaloniki, Greece: Intercomparison and validation of two inversion algorithms. *Atmos. Meas. Tech.* **2022**, *15*, 1269–1301. [[CrossRef](#)]
63. Kalivitis, N.; Gerasopoulos, E.; Vrekoussis, M.; Kouvarakis, G.; Kubilay, N.; Hatzianastassiou, N.; Vardavas, I.; Mihalopoulos, N. Dust transport over the eastern Mediterranean derived from Total Ozone Mapping Spectrometer, Aerosol Robotic Network, and surface measurements. *J. Geophys. Res. Atmos.* **2007**, *112*, D03202. [[CrossRef](#)]
64. Kelektsgolou, K.; Rapsomanikis, S. AERONET observations of direct and indirect aerosol effects over a South European conurbation. *Int. J. Remote Sens.* **2011**, *32*, 2779–2798. [[CrossRef](#)]

65. Kazadzis, S.; Bais, A.; Amiridis, V.; Balis, D.; Meleti, C.; Kouremeti, N.; Zerefos, C.S.; Rapsomanikis, S.; Petrakakis, M.; Kelesis, A.; et al. Nine years of UV aerosol optical depth measurements at Thessaloniki, Greece. *Atmos. Chem. Phys.* **2007**, *7*, 2091–2101. [[CrossRef](#)]
66. Kazadzis, S.; Veselovskii, I.; Amiridis, V.; Gröbner, J.; Suvorina, A.; Nyeki, S.; Gerasopoulos, E.; Kouremeti, N.; Taylor, M.; Tsekeris, A.; et al. Aerosol microphysical retrievals from precision filter radiometer direct solar radiation measurements and comparison with AERONET. *Atmos. Meas. Tech.* **2014**, *7*, 2013–2025. [[CrossRef](#)]
67. Kazadzis, S.; Raptis, P.I.; Kouremeti, N.; Amiridis, V.; Arola, A.; Gerasopoulos, E.; Schuster, G.L. Aerosol Absorption Retrieval at Ultraviolet Wavelengths in Acomplex Environment. *Atmos. Meas. Tech.* **2016**, *9*, 5997–6011. [[CrossRef](#)]
68. Raptis, I.-P.; Kazadzis, S.; Amiridis, V.; Gkikas, A.; Gerasopoulos, E.; Mihalopoulos, N. A Decade of Aerosol Optical Properties Measurements over Athens, Greece. *Atmosphere* **2020**, *11*, 154. [[CrossRef](#)]
69. Siomos, N.; Fountoulakis, I.; Natsis, A.; Drosoglou, T.; Bais, A. Automated Aerosol Classification from Spectral UV Measurements Using Machine Learning Clustering. *Remote Sens.* **2020**, *12*, 965. [[CrossRef](#)]
70. Kazadzis, S.; Bais, A.; Kouremeti, N.; Gerasopoulos, E.; Garane, K.; Blumthaler, M.; Schallhart, B.; Cede, A. Direct spectral measurements with a Brewer spectroradiometer: Absolute calibration and aerosol optical depth retrieval. *Appl. Opt.* **2005**, *44*, 1681. [[CrossRef](#)]
71. Kazadzis, S.; Kouremeti, N.; Bais, A.; Kazantzidis, A.; Meleti, C. Aerosol forcing efficiency in the UVA region from spectral solar irradiance measurements at an urban environment. *Ann. Geophys.* **2009**, *27*, 2515–2522. [[CrossRef](#)]
72. Bais, A.F. Absolute spectral measurements of direct solar ultraviolet irradiance with a Brewer spectrophotometer. *Appl. Opt.* **1997**, *36*, 5199. [[CrossRef](#)]
73. Bais, A.F.; Kazantzidis, A.; Kazadzis, S.; Balis, D.S.; Zerefos, C.S.; Meleti, C. Deriving an effective aerosol single scattering albedo from spectral surface UV irradiance measurements. *Atmos. Environ.* **2005**, *39*, 1093–1102. [[CrossRef](#)]
74. Fountoulakis, I.; Natsis, A.; Siomos, N.; Drosoglou, T.; Bais, A.F. Deriving Aerosol Absorption Properties from Solar Ultraviolet Radiation Spectral Measurements at Thessaloniki, Greece. *Remote Sens.* **2019**, *11*, 2179. [[CrossRef](#)]
75. Masoom, A.; Fountoulakis, I.; Kazadzis, S.; Raptis, I.-P.; Kampouri, A.; Psiloglou, B.E.; Kouklaki, D.; Papachristopoulou, K.; Marinou, E.; Solomos, S.; et al. Investigation of the effects of the Greek extreme wildfires of August 2021 on air quality and spectral solar irradiance. *Atmos. Chem. Phys.* **2023**, *23*, 8487–8514. [[CrossRef](#)]
76. Gerasopoulos, E.; Kokkalis, P.; Amiridis, V.; Liakakou, E.; Perez, C.; Haustein, K.; Eleftheratos, K.; Andreae, M.O.; Andreae, T.W.; Zerefos, C.S. Dust specific extinction cross-sections over the Eastern Mediterranean using the BSC-DREAM model and sun photometer data: The case of urban environments. *Ann. Geophys.* **2009**, *27*, 2903–2912. [[CrossRef](#)]
77. Gerasopoulos, E.; Amiridis, V.; Kazadzis, S.; Kokkalis, P.; Eleftheratos, K.; Andreae, M.O.; Andreae, T.W.; El-Askary, H.; Zerefos, C.S. Three-year ground based measurements of aerosol optical depth over the Eastern Mediterranean: The urban environment of Athens. *Atmos. Chem. Phys.* **2011**, *11*, 2145–2159. [[CrossRef](#)]
78. Raptis, I.-P.; Kazadzis, S.; Eleftheratos, K.; Amiridis, V.; Fountoulakis, I. Single Scattering Albedo’s Spectral Dependence Effect on UV Irradiance. *Atmosphere* **2018**, *9*, 364. [[CrossRef](#)]
79. Tsaknakis, G.; Papayannis, A.; Kokkalis, P.; Amiridis, V.; Kambezidis, H.D.; Mamouri, R.E.; Georgouassis, G.; Avdikos, G. Inter-comparison of lidar and ceilometer retrievals for aerosol and Planetary Boundary Layer profiling over Athens, Greece. *Atmos. Meas. Tech.* **2011**, *4*, 1261–1273. [[CrossRef](#)]
80. Kambezidis, H.D.; Psiloglou, B.E.; Gavriil, A.; Petrinoli, K. Detection of Upper and Lower Planetary-Boundary Layer Curves and Estimation of Their Heights from Ceilometer Observations under All-Weather Conditions: Case of Athens, Greece. *Remote Sens.* **2021**, *13*, 2175. [[CrossRef](#)]
81. Pappalardo, G.; Amodeo, A.; Apituley, A.; Comeron, A.; Freudenthaler, V.; Linné, H.; Ansmann, A.; Bösenberg, J.; D’Amico, G.; Mattis, I.; et al. EARLINET: Towards an advanced sustainable European aerosol lidar network. *Atmos. Meas. Tech.* **2014**, *7*, 2389–2409. [[CrossRef](#)]
82. Available online: <http://pre-tect.space.noa.gr/> (accessed on 20 May 2024).
83. Available online: <https://calishto.panacea-ri.gr/> (accessed on 22 May 2024).
84. Zerefos, C.S.; Kourtidis, K.A.; Melas, D.; Balis, D.; Zanis, P.; Katsaros, L.; Mantis, H.T.; Repapis, C.; Isaksen, I.; Sundet, J.; et al. Photochemical Activity and Solar Ultraviolet Radiation (PAUR) Modulation Factors: An overview of the project. *J. Geophys. Res. Atmos.* **2002**, *107*, PAU 1-1–PAU 1-15. [[CrossRef](#)]
85. Logothetis, S.-A.; Salamatikis, V.; Kazantzidis, A. Aerosol classification in Europe, Middle East, North Africa and Arabian Peninsula based on AERONET Version 3. *Atmos. Res.* **2020**, *239*, 104893. [[CrossRef](#)]
86. Monteiro, A.; Basart, S.; Kazadzis, S.; Votsis, A.; Gkikas, A.; Vandebussche, S.; Tobias, A.; Gama, C.; García-Pando, C.P.; Terradellas, E.; et al. Multi-sectoral impact assessment of an extreme African dust episode in the Eastern Mediterranean in March 2018. *Sci. Total. Environ.* **2022**, *843*, 156861. [[CrossRef](#)]
87. Turquety, S.; Hurtmans, D.; Hadji-Lazaro, J.; Coheur, P.-F.; Clerbaux, C.; Josset, D.; Tsamalis, C. Tracking the emission and transport of pollution from wildfires using the IASI CO retrievals: Analysis of the summer 2007 Greek fires. *Atmos. Chem. Phys.* **2009**, *9*, 4897–4913. [[CrossRef](#)]
88. Amiridis, V.; Zerefos, C.; Kazadzis, S.; Gerasopoulos, E.; Eleftheratos, K.; Vrekoussis, M.; Stohl, A.; Mamouri, R.E.; Kokkalis, P.; Papayannis, A.; et al. Impact of the 2009 Attica wild fires on the air quality in urban Athens. *Atmos. Environ.* **2012**, *46*, 536–544. [[CrossRef](#)]

89. Poupkou, A.; Markakis, K.; Liora, N.; Giannaros, T.M.; Zanis, P.; Im, U.; Daskalakis, N.; Myriokefalitakis, S.; Kaiser, J.W.; Melas, D.; et al. A modeling study of the impact of the 2007 Greek forest fires on the gaseous pollutant levels in the Eastern Mediterranean. *Atmos. Res.* **2014**, *149*, 1–17. [[CrossRef](#)]
90. Balis, D.S.; Amiridis, V.; Zerefos, C.; Gerasopoulos, E.; Andreae, M.; Zanis, P.; Kazantzidis, A.; Kazadzis, S.; Papayannis, A. Raman lidar and sunphotometric measurements of aerosol optical properties over Thessaloniki, Greece during a biomass burning episode. *Atmos. Environ.* **2003**, *37*, 4529–4538. [[CrossRef](#)]
91. Amiridis, V.; Giannakaki, E.; Balis, D.S.; Gerasopoulos, E.; Pytharoulis, I.; Zanis, P.; Kazadzis, S.; Melas, D.; Zerefos, C. Smoke injection heights from agricultural burning in Eastern Europe as seen by CALIPSO. *Atmos. Chem. Phys.* **2010**, *10*, 11567–11576. [[CrossRef](#)]
92. Gkikas, A.; Houssos, E.E.; Hatzianastassiou, N.; Papadimas, C.D.; Bartzokas, A. Synoptic conditions favouring the occurrence of aerosol episodes over the broader Mediterranean basin. *Q. J. R. Meteorol. Soc.* **2012**, *138*, 932–949. [[CrossRef](#)]
93. Papanikolaou, C.-A.; Giannakaki, E.; Papayannis, A.; Mylonaki, M.; Soupiona, O. Canadian Biomass Burning Aerosol Properties Modification during a Long-Ranged Event on August 2018. *Sensors* **2020**, *20*, 5442. [[CrossRef](#)]
94. Baars, H.; Radenz, M.; Floutsi, A.A.; Engelmann, R.; Althausen, D.; Heese, B.; Ansmann, A.; Flament, T.; Dabas, A.; Trapou, D.; et al. Californian Wildfire Smoke Over Europe: A First Example of the Aerosol Observing Capabilities of Aeolus Compared to Ground-Based Lidar. *Geophys. Res. Lett.* **2021**, *48*, e2020GL092194. [[CrossRef](#)]
95. Zerefos, C.S.; Gerogiannis, V.T.; Balis, D.; Zerefos, S.C.; Kazantzidis, A. Atmospheric effects of volcanic eruptions as seen by famous artists and depicted in their paintings. *Atmos. Chem. Phys.* **2007**, *7*, 4027–4042. [[CrossRef](#)]
96. Pappalardo, G.; Wandinger, U.; Mona, L.; Hiebsch, A.; Mattis, I.; Amodeo, A.; Ansmann, A.; Seifert, P.; Linné, H.; Apituley, A.; et al. EARLINET correlative measurements for CALIPSO: First intercomparison results. *J. Geophys. Res. Atmos.* **2010**, *115*, 2009JD012147. [[CrossRef](#)]
97. Kampouri, A.; Amiridis, V.; Solomos, S.; Gialitaki, A.; Marinou, E.; Spyrou, C.; Georgoulias, A.K.; Akritidis, D.; Papagiannopoulos, N.; Mona, L.; et al. Investigation of Volcanic Emissions in the Mediterranean: “The Etna–Antikythera Connection”. *Atmosphere* **2021**, *12*, 40. [[CrossRef](#)]
98. Amiridis, V.; Kampouri, A.; Gkikas, A.; Misios, S.; Gialitaki, A.; Marinou, E.; Rennie, M.; Benedetti, A.; Solomos, S.; Zanis, P.; et al. Aeolus winds impact on volcanic ash early warning systems for aviation. *Sci. Rep.* **2023**, *13*, 7531. [[CrossRef](#)]
99. Varlas, G.; Marinou, E.; Gialitaki, A.; Siomos, N.; Tsarpalis, K.; Kalivitis, N.; Solomos, S.; Tsekeli, A.; Spyrou, C.; Tsichla, M.; et al. Assessing Sea-State Effects on Sea-Salt Aerosol Modeling in the Lower Atmosphere Using Lidar and In-Situ Measurements. *Remote Sens.* **2021**, *13*, 614. [[CrossRef](#)]
100. Syrigou, E.; Zanikou, S.; Papageorgiou, P.S. Grasses, olive, parietaria and cypress in Athens: Pollen sampling from 1995 to 1999. *Aerobiologia* **2003**, *19*, 133–137. [[CrossRef](#)]
101. Gioulekas, D.; Damialis, A.; Papakosta, D.; Syrigou, A.; Mpaka, G.; Saxon, F.; Patakas, D. 15-Year aeroallergen records. Their usefulness in Athens Olympics, 2004. *Allergy* **2003**, *58*, 933–938. [[CrossRef](#)] [[PubMed](#)]
102. Pyrri, I.; Kapsanaki-Gotsi, E. Diversity and annual fluctuations of culturable airborne fungi in Athens, Greece: A 4-year study. *Aerobiologia* **2012**, *28*, 249–262. [[CrossRef](#)]
103. Pyrri, I.; Kapsanaki-Gotsi, E. Evaluation of the fungal aerosol in Athens, Greece, based on spore analysis. *Aerobiologia* **2015**, *31*, 179–190. [[CrossRef](#)]
104. Richardson, S.C.; Mytilinaios, M.; Foskinis, R.; Kyrou, C.; Papayannis, A.; Pyrri, I.; Giannoutsou, E.; Adamakis, I.D.S. Bioaerosol detection over Athens, Greece using the laser induced fluorescence technique. *Sci. Total. Environ.* **2019**, *696*, 133906. [[CrossRef](#)]
105. Hess, M.; Koepke, P.; Schult, I. Optical Properties of Aerosols and Clouds: The Software Package OPAC. *Bull. Amer. Meteor. Soc.* **1998**, *79*, 831–844. [[CrossRef](#)]
106. Dubovik, O.; Holben, B.; Eck, T.F.; Smirnov, A.; Kaufman, Y.J.; King, M.D.; Tanré, D.; Slutsker, I. Variability of Absorption and Optical Properties of Key Aerosol Types Observed in Worldwide Locations. *J. Atmos. Sci.* **2002**, *59*, 590–608. [[CrossRef](#)]
107. Available online: <https://www.caelis.uva.es/> (accessed on 22 May 2024).
108. Nastos, P.T. Meteorological Patterns Associated with Intense Saharan Dust Outbreaks over Greece in Winter. *Adv. Meteorol.* **2012**, *2012*, 828301. [[CrossRef](#)]
109. Solomos, S.; Kalivitis, N.; Mihalopoulos, N.; Amiridis, V.; Kouvarakis, G.; Gkikas, A.; Binietoglou, I.; Tsekeli, A.; Kazadzis, S.; Kottas, M.; et al. From Tropospheric Folding to Khamsin and Foehn Winds: How Atmospheric Dynamics Advanced a Record-Breaking Dust Episode in Crete. *Atmosphere* **2018**, *9*, 240. [[CrossRef](#)]
110. Kaskaoutis, D.G.; Rashki, A.; Dumka, U.C.; Mofidi, A.; Kambezidis, H.D.; Psiloglou, B.E.; Karagiannis, D.; Petrinoli, K.; Gavril, A. Atmospheric dynamics associated with exceptionally dusty conditions over the eastern Mediterranean and Greece in March 2018. *Atmos. Res.* **2019**, *218*, 269–284. [[CrossRef](#)]
111. Georgoulias, A.K.; Tsikerdekis, A.; Amiridis, V.; Marinou, E.; Benedetti, A.; Zanis, P.; Alexandri, G.; Mona, L.; Kourtidis, K.A.; Lelieveld, J. A 3-D evaluation of the MACC reanalysis dust product over Europe, northern Africa and Middle East using CALIOP/CALIPSO dust satellite observations. *Atmos. Chem. Phys.* **2018**, *18*, 8601–8620. [[CrossRef](#)]
112. Gkikas, A.; Basart, S.; Hatzianastassiou, N.; Marinou, E.; Amiridis, V.; Kazadzis, S.; Pey, J.; Querol, X.; Jorba, O.; Gassó, S.; et al. Mediterranean intense desert dust outbreaks and their vertical structure based on remote sensing data. *Atmos. Chem. Phys.* **2016**, *16*, 8609–8642. [[CrossRef](#)]

113. Amiridis, V.; Marinou, E.; Tsekeli, A.; Wandinger, U.; Schwarz, A.; Giannakaki, E.; Mamouri, R.; Kokkalis, P.; Binietoglou, I.; Solomos, S.; et al. LIVAS: A 3-D multi-wavelength aerosol/cloud database based on CALIPSO and EARLINET. *Atmos. Chem. Phys.* **2015**, *15*, 7127–7153. [[CrossRef](#)]
114. Balis, D.; Papayannis, A.; Galani, E.; Marenco, F.; Santacesaria, V.; Hamonou, E.; Chazette, P.; Ziomas, I.; Zerefos, C. Tropospheric LIDAR aerosol measurements and sun photometric observations at Thessaloniki, Greece. *Atmos. Environ.* **2000**, *34*, 925–932. [[CrossRef](#)]
115. Gerasopoulos, E.; Andreae, M.O.; Zerefos, C.S.; Andreae, T.W.; Balis, D.; Formenti, P.; Merlet, P.; Amiridis, V.; Papastefanou, C. Climatological aspects of aerosol optical properties in Northern Greece. *Atmos. Chem. Phys.* **2003**, *3*, 2025–2041. [[CrossRef](#)]
116. Fotiadi, A.; Hatzianastassiou, N.; Drakakis, E.; Matsoukas, C.; Pavlakis, K.G.; Hatzidimitriou, D.; Gerasopoulos, E.; Mihalopoulos, N.; Vardavas, I. Aerosol physical and optical properties in the Eastern Mediterranean Basin, Crete, from Aerosol Robotic Network data. *Atmos. Chem. Phys.* **2006**, *6*, 5399–5413. [[CrossRef](#)]
117. Tsekeli, A.; Lopatin, A.; Amiridis, V.; Marinou, E.; Igloffstein, J.; Siomos, N.; Solomos, S.; Kokkalis, P.; Engelmann, R.; Baars, H.; et al. GARRLiC and LIRIC: Strengths and limitations for the characterization of dust and marine particles along with their mixtures. *Atmos. Meas. Tech.* **2017**, *10*, 4995–5016. [[CrossRef](#)]
118. Michailidis, K.; Koukouli, M.-E.; Balis, D.; Veefkind, J.P.; De Graaf, M.; Mona, L.; Papagianopoulos, N.; Pappalardo, G.; Tsikoudi, I.; Amiridis, V.; et al. Validation of the TROPOMI/S5P aerosol layer height using EARLINET lidars. *Atmos. Chem. Phys.* **2023**, *23*, 1919–1940. [[CrossRef](#)]
119. Konsta, D.; Tsekeli, A.; Solomos, S.; Siomos, N.; Gialitaki, A.; Tetoni, E.; Lopatin, A.; Goloub, P.; Dubovik, O.; Amiridis, V.; et al. The Potential of GRASP/GARRLiC Retrievals for Dust Aerosol Model Evaluation: Case Study during the PreTECT Campaign. *Remote Sens.* **2021**, *13*, 873. [[CrossRef](#)]
120. Marinou, E.; Voudouri, K.A.; Tsikoudi, I.; Drakaki, E.; Tsekeli, A.; Rosoldi, M.; Ene, D.; Baars, H.; O’Connor, E.; Amiridis, V.; et al. Geometrical and Microphysical Properties of Clouds Formed in the Presence of Dust above the Eastern Mediterranean. *Remote Sens.* **2021**, *13*, 5001. [[CrossRef](#)]
121. Solomos, S.; Amiridis, V.; Zanis, P.; Gerasopoulos, E.; Sofiou, F.I.; Herekakis, T.; Brioude, J.; Stohl, A.; Kahn, R.A.; Kontoes, C. Smoke dispersion modeling over complex terrain using high resolution meteorological data and satellite observations—The FireHub platform. *Atmos. Environ.* **2015**, *119*, 348–361. [[CrossRef](#)]
122. Solomos, S.; Gialitaki, A.; Marinou, E.; Proestakis, E.; Amiridis, V.; Baars, H.; Komppula, M.; Ansmann, A. Modeling and remote sensing of an indirect Pyro-Cb formation and biomass transport from Portugal wildfires towards Europe. *Atmos. Environ.* **2019**, *206*, 303–315. [[CrossRef](#)]
123. Van Der Werf, G.R.; Randerson, J.T.; Giglio, L.; Collatz, G.J.; Mu, M.; Kasibhatla, P.S.; Morton, D.C.; DeFries, R.S.; Jin, Y.; Van Leeuwen, T.T. Global fire emissions and the contribution of deforestation, savanna, forest, agricultural, and peat fires (1997–2009). *Atmos. Chem. Phys.* **2010**, *10*, 11707–11735. [[CrossRef](#)]
124. Available online: <http://smoke.beyond-eocenter.eu/> (accessed on 22 May 2024).
125. Van Der Werf, G.R.; Randerson, J.T.; Giglio, L.; Van Leeuwen, T.T.; Chen, Y.; Rogers, B.M.; Mu, M.; Van Marle, M.J.E.; Morton, D.C.; Collatz, G.J.; et al. Global fire emissions estimates during 1997–2016. *Earth Syst. Sci. Data* **2017**, *9*, 697–720. [[CrossRef](#)]
126. Baars, H.; Ansmann, A.; Althausen, D.; Engelmann, R.; Heese, B.; Müller, D.; Artaxo, P.; Paixao, M.; Pauliquevis, T.; Souza, R. Aerosol profiling with lidar in the Amazon Basin during the wet and dry season. *J. Geophys. Res. Atmos.* **2012**, *117*, 2012JD018338. [[CrossRef](#)]
127. Giannakaki, E.; Van Zyl, P.G.; Müller, D.; Balis, D.; Komppula, M. Optical and microphysical characterization of aerosol layers over South Africa by means of multi-wavelength depolarization and Raman lidar measurements. *Atmos. Chem. Phys.* **2016**, *16*, 8109–8123. [[CrossRef](#)]
128. Papanikolaou, C.-A.; Papayannis, A.; Mylonaki, M.; Foskinis, R.; Kokkalis, P.; Liakakou, E.; Stavroulas, I.; Soupiona, O.; Hatzianastassiou, N.; Gavrouzou, M.; et al. Vertical Profiling of Fresh Biomass Burning Aerosol Optical Properties over the Greek Urban City of Ioannina, during the PANACEA Winter Campaign. *Atmosphere* **2022**, *13*, 94. [[CrossRef](#)]
129. Baars, H.; Ansmann, A.; Ohneiser, K.; Haarig, M.; Engelmann, R.; Althausen, D.; Hanssen, I.; Gausa, M.; Pietruczuk, A.; Szkop, A.; et al. The unprecedented 2017–2018 stratospheric smoke event: Decay phase and aerosol properties observed with the EARLINET. *Atmos. Chem. Phys.* **2019**, *19*, 15183–15198. [[CrossRef](#)]
130. Rizza, U.; Canepa, E.; Miglietta, M.M.; Passerini, G.; Morichetti, M.; Mancinelli, E.; Virgili, S.; Besio, G.; De Leo, F.; Mazzino, A. Evaluation of drag coefficients under medicane conditions: Coupling waves, sea spray and surface friction. *Atmos. Res.* **2021**, *247*, 105207. [[CrossRef](#)]
131. Lewis, R.; Schwartz, E. *Sea Salt Aerosol Production: Mechanisms, Methods, Measurements and Models—A Critical Review*; American Geophysical Union: Washington, DC, USA, 2004; Volume 152. [[CrossRef](#)]
132. Haarig, M.; Ansmann, A.; Gasteiger, J.; Kandler, K.; Althausen, D.; Baars, H.; Radenz, M.; Farrell, D.A. Dry versus wet marine particle optical properties: RH dependence of depolarization ratio, backscatter, and extinction from multiwavelength lidar measurements during SALTRACE. *Atmos. Chem. Phys.* **2017**, *17*, 14199–14217. [[CrossRef](#)]
133. Mihalopoulos, N.; Stephanou, E.; Kanakidou, M.; Pilitsidis, S.; Bousquet, P. Tropospheric aerosol ionic composition in the Eastern Mediterranean region. *Tellus B* **1997**, *49*, 314–326. [[CrossRef](#)]
134. Lelieveld, J.; Berresheim, H.; Borrmann, S.; Crutzen, P.J.; Dentener, F.J.; Fischer, H.; Feichter, J.; Flatau, P.J.; Heland, J.; Holzinger, R.; et al. Global Air Pollution Crossroads over the Mediterranean. *Science (1979)* **2002**, *298*, 794–799. [[CrossRef](#)]

135. Regayre, L.A.; Schmale, J.; Johnson, J.S.; Tatzelt, C.; Baccarini, A.; Henning, S.; Yoshioka, M.; Stratmann, F.; Gysel-Beer, M.; Grosvenor, D.P.; et al. The value of remote marine aerosol measurements for constraining radiative forcing uncertainty. *Atmos. Chem. Phys.* **2020**, *20*, 10063–10072. [[CrossRef](#)]
136. Robock, A. Climatic impact of volcanic emissions. In *Geophysical Monograph Series*; Sparks, R.S.J., Hawkesworth, C.J., Eds.; American Geophysical Union: Washington, DC, USA, 2004; Volume 150, pp. 125–134. [[CrossRef](#)]
137. Ewert, J.W.; Guffanti, M.; Murray, T.L. *An Assessment of Volcanic Threat and Monitoring Capabilities in the United States: Framework for a National Volcano Early Warning System*; US Geological Survey: Reston, VA, USA, 2005.
138. Durant, A.J.; Bonadonna, C.; Horwell, C.J. Atmospheric and Environmental Impacts of Volcanic Particulates. *Elements* **2010**, *6*, 235–240. [[CrossRef](#)]
139. Thorsteinsson, T.; Jóhannsson, T.; Stohl, A.; Kristiansen, N.I. High levels of particulate matter in Iceland due to direct ash emissions by the Eyjafjallajökull eruption and resuspension of deposited ash. *J. Geophys. Res. Solid. Earth* **2012**, *117*, 2011JB008756. [[CrossRef](#)]
140. Reichardt, U.; Ulfarsson, G.F.; Pétursdóttir, G. Volcanic ash and aviation: Recommendations to improve preparedness for extreme events. *Transp. Res. Part. A Policy Pract.* **2018**, *113*, 101–113. [[CrossRef](#)]
141. Mastin, L.; Pavoloni, M.; Engwell, S.; Clarkson, R.; Witham, C.; Brock, G.; Lisk, I.; Guffanti, M.; Tupper, A.; Schneider, D.; et al. Progress in protecting air travel from volcanic ash clouds. *Bull. Volcanol.* **2022**, *84*, 9. [[CrossRef](#)]
142. Volcanic ash Contingency Plan-European and North Atlantic Regions EUR/NAT VACP Edition 2.2.0-January 2024 This Document Is Issued by the EUR/NAT OFFICE OF ICAO under the Authority of the EASPG and the NAT SPG. Available online: https://www.icao.int/EURNAT/Pages/METEOROLOGY/Volc_Ash_CPs.aspx (accessed on 22 May 2024).
143. Calabrese, S.; Aiuppa, A.; Allard, P.; Bagnato, E.; Bellomo, S.; Brusca, L.; D’Alessandro, W.; Parello, F. Atmospheric sources and sinks of volcanogenic elements in a basaltic volcano (Etna, Italy). *Geochim. Cosmochim. Acta* **2011**, *75*, 7401–7425. [[CrossRef](#)]
144. Brugnone, F.; D’Alessandro, W.; Calabrese, S.; Li Vigni, L.; Bellomo, S.; Brusca, L.; Prano, V.; Saiano, F.; Parello, F. A Christmas gift: Signature of the 24th December 2018 eruption of Mt. Etna on the chemical composition of bulk deposition in eastern Sicily. *Ital. J. Geosci.* **2020**, *139*, 341–358. [[CrossRef](#)]
145. Wang, X.; Boselli, A.; D’Avino, L.; Pisani, G.; Spinelli, N.; Amodeo, A.; Chaikovsky, A.; Wiegner, M.; Nickovic, S.; Papayannis, A.; et al. Volcanic dust characterization by EARLINET during Etna’s eruptions in 2001–2002. *Atmos. Environ.* **2008**, *42*, 893–905. [[CrossRef](#)]
146. Ansmann, A.; Frunke, J.; Engelmann, R. Updraft and downdraft characterization with Doppler lidar: Cloud-free versus cumuli-topped mixed layer. *Atmos. Chem. Phys.* **2010**, *10*, 7845–7858. [[CrossRef](#)]
147. Balis, D.; Koukouli, M.-E.; Siomos, N.; Dimopoulos, S.; Mona, L.; Pappalardo, G.; Marenco, F.; Clarisse, L.; Ventress, L.J.; Carboni, E.; et al. Validation of ash optical depth and layer height retrieved from passive satellite sensors using EARLINET and airborne lidar data: The case of the Eyjafjallajökull eruption. *Atmos. Chem. Phys.* **2016**, *16*, 5705–5720. [[CrossRef](#)]
148. Schmidt, C.W. Pollen Overload: Seasonal Allergies in a Changing Climate. *Environ. Health Perspect.* **2016**, *124*, A70–A75. [[CrossRef](#)]
149. Ziska, L.H.; Beggs, P.J. Anthropogenic climate change and allergen exposure: The role of plant biology. *J. Allergy Clin. Immunol.* **2012**, *129*, 27–32. [[CrossRef](#)]
150. Mandrioli, P.; Negrini, M.G.; Cesari, G.; Morgan, G. Evidence for long range transport of biological and anthropogenic aerosol particles in the atmosphere. *Grana* **1984**, *23*, 43–53. [[CrossRef](#)]
151. Rousseau, D.; Schevin, P.; Ferrier, J.; Jolly, D.; Andreasen, T.; Ascanius, S.E.; Hendriksen, S.; Poulsen, U. Long-distance pollen transport from North America to Greenland in spring. *J. Geophys. Res. Biogeosci.* **2008**, *113*, 2007JG000456. [[CrossRef](#)]
152. Skjøth, C.A.; Sommer, J.; Stach, A.; Smith, M.; Brandt, J. The long-range transport of birch (*Betula*) pollen from Poland and Germany causes significant pre-season concentrations in Denmark. *Clin. Exp. Allergy* **2007**, *37*, 1204–1212. [[CrossRef](#)]
153. Szczepanek, K.; Myszkowska, D.; Worobiec, E.; Piotrowicz, K.; Ziemanin, M.; Bielec-Bąkowska, Z. The long-range transport of Pinaceae pollen: An example in Kraków (southern Poland). *Aerobiologia* **2017**, *33*, 109–125. [[CrossRef](#)]
154. Von Blohn, N.; Mitra, S.K.; Diehl, K.; Borrmann, S. The ice nucleating ability of pollen. *Atmos. Res.* **2005**, *78*, 182–189. [[CrossRef](#)]
155. Diehl, K.; Quick, C.; Matthias-Maser, S.; Mitra, S.K.; Jaenicke, R. The ice nucleating ability of pollen. *Atmos. Res.* **2001**, *58*, 75–87. [[CrossRef](#)]
156. Diehl, K.; Matthias-Maser, S.; Jaenicke, R.; Mitra, S.K. The ice nucleating ability of pollen. *Atmos. Res.* **2002**, *61*, 125–133.
157. Steiner, A.L.; Brooks, S.D.; Deng, C.; Thornton, D.C.O.; Pendleton, M.W.; Bryant, V. Pollen as atmospheric cloud condensation nuclei. *Geophys. Res. Lett.* **2015**, *42*, 3596–3602. [[CrossRef](#)]
158. Wozniak, M.C.; Solmon, F.; Steiner, A.L. Pollen Rupture and Its Impact on Precipitation in Clean Continental Conditions. *Geophys. Res. Lett.* **2018**, *45*, 7156–7164. [[CrossRef](#)]
159. D’Amato, G.; Cecchi, L.; Bonini, S.; Nunes, C.; Annesi-Maesano, I.; Behrendt, H.; Liccardi, G.; Popov, T.; Van Cauwenbergh, P. Allergenic pollen and pollen allergy in Europe. *Allergy* **2007**, *62*, 976–990. [[CrossRef](#)]
160. Bohlmann, S.; Shang, X.; Giannakaki, E.; Filioglou, M.; Saarto, A.; Romakkaniemi, S.; Komppula, M. Detection and characterization of birch pollen in the atmosphere using a multiwavelength Raman polarization lidar and Hirst-type pollen sampler in Finland. *Atmos. Chem. Phys.* **2019**, *19*, 14559–14569. [[CrossRef](#)]

161. Shang, X.; Giannakaki, E.; Bohlmann, S.; Filioglou, M.; Saarto, A.; Ruuskanen, A.; Leskinen, A.; Romakkaniemi, S.; Komppula, M. Optical characterization of pure pollen types using a multi-wavelength Raman polarization lidar. *Atmos. Chem. Phys.* **2020**, *20*, 15323–15339. [[CrossRef](#)]
162. Dobson, G.M.B. A photoelectric spectrophotometer for measuring the amount of atmospheric ozone. *Proc. Phys. Soc.* **1931**, *43*, 324–339. [[CrossRef](#)]
163. Bais, A.; Tourpali, K.; Kelessis, A.; Ziomas, I.; Zerefos, C.; Amanatidis, G. Six years of regular ozone observations with a Brewer Spectrophotometer at Thessaloniki, Greece. In Proceedings of the Quadrennial Ozone Symposium, Göttingen, Germany, 4–13 August 1988.
164. Bais, A.F.; Tourpali, K.D.; Zerefos, C.S.; Ziomas, I.C. Reply to the paper: On the total ozone depletion over Greece derived from satellite flown and ground-based instruments. *Int. J. Remote Sens.* **1994**, *15*, 3295–3301. [[CrossRef](#)]
165. Zerefos, C.S.; Balis, D.S.; Bais, A.F.; Gillotay, D.; Simon, P.C.; Mayer, B.; Seckmeyer, G. Variability of UV-B at four stations in Europe. *Geophys. Res. Lett.* **1997**, *24*, 1363–1366. [[CrossRef](#)]
166. Zerefos, C.; Meleti, C.; Balis, D.; Tourpali, K.; Bais, A.F. Quasi-biennial and longer-term changes in clear sky UV-B solar irradiance. *Geophys. Res. Lett.* **1998**, *25*, 4345–4348. [[CrossRef](#)]
167. Zerefos, C.S. Long-term ozone and UV variations at Thessaloniki, Greece. *Phys. Chem. Earth Parts A/B/C* **2002**, *27*, 455–460. [[CrossRef](#)]
168. Varotsos, C.A.; Cracknell, A.P. Ozone depletion over Greece as deduced from Nimbus-7 TOMS measurements. *Int. J. Remote Sens.* **1993**, *14*, 2053–2059. [[CrossRef](#)]
169. Varotsos, C.A. Total ozone depletion over Greece as deduced from satellite observations. *Int. J. Remote Sens.* **1998**, *19*, 3317–3325. [[CrossRef](#)]
170. Varotsos, C.A.; Kondratyev, K.Y.; Cracknell, A.P. New evidence for ozone depletion over Athens, Greece. *Int. J. Remote Sens.* **2000**, *21*, 2951–2955. [[CrossRef](#)]
171. Garane, K.; Bais, A.F.; Kazadzis, S.; Kazantzidis, A.; Meleti, C. Monitoring of UV spectral irradiance at Thessaloniki (1990–2005): Data re-evaluation and quality control. *Ann. Geophys.* **2006**, *24*, 3215–3228. [[CrossRef](#)]
172. Fountoulakis, I.; Bais, A.F.; Fragkos, K.; Meleti, C.; Tourpali, K.; Zempila, M.M. Short- and long-term variability of spectral solar UV irradiance at Thessaloniki, Greece: Effects of changes in aerosols, total ozone and clouds. *Atmos. Chem. Phys.* **2016**, *16*, 2493–2505. [[CrossRef](#)]
173. Fountoulakis, I.; Zerefos, C.S.; Bais, A.F.; Kapsomenakis, J.; Koukouli, M.-E.; Ohkawara, N.; Fioletov, V.; De Backer, H.; Lakkala, K.; Karppinen, T.; et al. Twenty-five years of spectral UV-B measurements over Canada, Europe and Japan: Trends and effects from changes in ozone, aerosols, clouds, and surface reflectivity. *Comptes Rendus. Géoscience* **2018**, *350*, 393–402. [[CrossRef](#)]
174. Meleti, C.; Bais, A.; Tourpali, K.; Balis, D.; Zerefos, C.; Fragkos, K. Thirty years of total ozone measurements at Thessaloniki with a MKII Brewer spectrophotometer. In Proceedings of the Quadrennial Ozone Symposium, Toronto, ON, Canada, 27–31 August 2012.
175. Zerefos, C.S.; Tourpali, K.; Eleftheratos, K.; Kazadzis, S.; Meleti, C.; Feister, U.; Koskela, T.; Heikkilä, A. Evidence of a possible turning point in solar UV-B over Canada, Europe and Japan. *Atmos. Chem. Phys.* **2012**, *12*, 2469–2477. [[CrossRef](#)]
176. Fountoulakis, I.; Redondas, A.; Bais, A.F.; Rodriguez-Franco, J.J.; Fragkos, K.; Cede, A. Dead time effect on the Brewer measurements: Correction and estimated uncertainties. *Atmos. Meas. Tech.* **2016**, *9*, 1799–1816. [[CrossRef](#)]
177. Garane, K.; Fountoulakis, I.; Karanikolas, A.; Bais, A.F.; Meleti, C. Thirty years of solar ultraviolet spectral irradiance measurements in Thessaloniki: Variability and trends. *AIP Conf. Proc.* **2024**, *2988*, 090003.
178. Fragkos, K.; Bais, A.F.; Fountoulakis, I.; Balis, D.; Tourpali, K.; Meleti, C.; Zanis, P. Extreme total column ozone events and effects on UV solar radiation at Thessaloniki, Greece. *Appl. Clim.* **2016**, *126*, 505–517. [[CrossRef](#)]
179. Available online: <https://lapweb.physics.auth.gr/> (accessed on 22 May 2024).
180. Eleftheratos, K.; Kouklaki, D.; Zerefos, C. Sixteen Years of Measurements of Ozone over Athens, Greece with a Brewer Spectrophotometer. *Oxygen* **2021**, *1*, 32–45. [[CrossRef](#)]
181. Koukouli, M.E.; Lerot, C.; Granville, J.; Goutail, F.; Lambert, J.-C.; Pommereau, J. -P.; Balis, D.; Zyrichidou, I.; Van Roozendael, M.; Coldewey-Egbers, M.; et al. Evaluating a new homogeneous total ozone climate data record from GOME/ERS-2, SCIAMACHY/Envisat, and GOME-2/MetOp-A. *J. Geophys. Res. Atmos.* **2015**, *120*, 12–296. [[CrossRef](#)]
182. Garane, K.; Lerot, C.; Coldewey-Egbers, M.; Verhoelst, T.; Koukouli, M.E.; Zyrichidou, I.; Balis, D.S.; Danckaert, T.; Goutail, F.; Granville, J.; et al. Quality assessment of the Ozone_cci Climate Research Data Package (release 2017)—Part 1: Ground-based validation of total ozone column data products. *Atmos. Meas. Tech.* **2018**, *11*, 1385–1402. [[CrossRef](#)]
183. Garane, K.; Koukouli, M.-E.; Verhoelst, T.; Lerot, C.; Heue, K.-P.; Fioletov, V.; Balis, D.; Bais, A.; Bazureau, A.; Dehn, A.; et al. TROPOMI/S5P total ozone column data: Global ground-based validation and consistency with other satellite missions. *Atmos. Meas. Tech.* **2019**, *12*, 5263–5287. [[CrossRef](#)]
184. Xing, J.; Wang, J.; Mathur, R.; Wang, S.; Sarwar, G.; Pleim, J.; Hogrefe, C.; Zhang, Y.; Jiang, J.; Wong, D.C.; et al. Impacts of aerosol direct effects on tropospheric ozone through changes in atmospheric dynamics and photolysis rates. *Atmos. Chem. Phys.* **2017**, *17*, 9869–9883. [[CrossRef](#)]
185. Zanis, P.; Hadjinicolaou, P.; Pozzer, A.; Tyrlis, E.; Dafka, S.; Mihalopoulos, N.; Lelieveld, J. Summertime free-tropospheric ozone pool over the eastern Mediterranean/Middle East. *Atmos. Chem. Phys.* **2014**, *14*, 115–132. [[CrossRef](#)]

186. Akritidis, D.; Pozzer, A.; Zanis, P.; Tyrlis, E.; Škerlak, B.; Sprenger, M.; Lelieveld, J. On the role of tropopause folds in summertime tropospheric ozone over the eastern Mediterranean and the Middle East. *Atmos. Chem. Phys.* **2016**, *16*, 14025–14039. [CrossRef]
187. Dafka, S.; Akritidis, D.; Zanis, P.; Pozzer, A.; Xoplaki, E.; Luterbacher, J.; Zerefos, C. On the link between the Etesian winds, tropopause folds and tropospheric ozone over the Eastern Mediterranean during summer. *Atmos. Res.* **2021**, *248*, 105161. [CrossRef]
188. Doche, C.; Dufour, G.; Foret, G.; Eremenko, M.; Cuesta, J.; Beekmann, M.; Kalabokas, P. Summertime tropospheric-ozone variability over the Mediterranean basin observed with IASI. *Atmos. Chem. Phys.* **2014**, *14*, 10589–10600. [CrossRef]
189. Myriokefalitakis, S.; Daskalakis, N.; Fanourgakis, G.S.; Voulgarakis, A.; Krol, M.C.; Aan De Brugh, J.M.J.; Kanakidou, M. Ozone and carbon monoxide budgets over the Eastern Mediterranean. *Sci. Total Environ.* **2016**, *563–564*, 40–52. [CrossRef]
190. Rizos, K.; Logothetis, I.; Koukouli, M.-E.; Meleti, C.; Melas, D. The influence of the summer tropospheric circulation on the observed ozone mixing ratios at a coastal site in the Eastern Mediterranean. *Atmos. Pollut. Res.* **2022**, *13*, 101381. [CrossRef]
191. Safieddine, S.; Boynard, A.; Coheur, P.-F.; Hurtmans, D.; Pfister, G.; Quennehen, B.; Thomas, J.L.; Raut, J.-C.; Law, K.S.; Klimont, Z.; et al. Summertime tropospheric ozone assessment over the Mediterranean region using the thermal infrared IASI/MetOp sounder and the WRF-Chem model. *Atmos. Chem. Phys.* **2014**, *14*, 10119–10131. [CrossRef]
192. Available online: <https://giovanni.gsfc.nasa.gov/> (accessed on 22 May 2024).
193. Georgoulias, A.K.; Kourtidis, K.A.; Buchwitz, M.; Schneising, O.; Burrows, J.P. A case study on the application of SCIAMACHY satellite methane measurements for regional studies: The Greater Area of the Eastern Mediterranean. *Int. J. Remote Sens.* **2011**, *32*, 787–813. [CrossRef]
194. Kourtidis, K.; Tzivleris, A.; Stathopoulos, S.; Gemitzi, A.; Georgoulias, A.K. On the Methane Emissions of the Greater Thessaloniki Area. *Environ. Sci. Proc.* **2023**, *26*, 39. [CrossRef]
195. Mermigkas, M.; Topaloglou, C.; Balis, D.; Koukouli, M.E.; Hase, F.; Dubravica, D.; Borsdorff, T.; Lorente, A. FTIR Measurements of Greenhouse Gases over Thessaloniki, Greece in the Framework of COCCON and Comparison with S5P/TROPOMI Observations. *Remote Sens.* **2021**, *13*, 3395. [CrossRef]
196. Mermigkas, M.; Topaloglou, C.; Koukouli, M.-E.; Balis, D.; Hase, F.; Dubravica, D.; Borsdorff, T.; Lorente, A. Sentinel-5P/TROPOspheric Monitoring Instrument CH₄ and CO Total Column Validation over the Thessaloniki Collaborative Carbon Column Observing Network Site, Greece. *Environ. Sci. Proc.* **2023**, *26*, 188. [CrossRef]
197. Copernicus Climate Change Service (C3S). *European State of the Climate 2022*; Copernicus Climate Change Service (C3S): Bologna, Italy, 2023. [CrossRef]
198. Cloud Properties-LAADS DAAC (nasa.gov). Available online: <https://ladsweb.modaps.eosdis.nasa.gov/missions-and-measurements/science-domain/cloud/> (accessed on 24 May 2024).
199. Georgoulias, A.K.; Boersma, K.F.; Van Vliet, J.; Zhang, X.; Zanis, P.; de Laat, J. Detection of NO₂ pollution plumes from individual ships with the TROPOMI/S5P satellite sensor. *Environ. Res. Lett.* **2020**, *15*, 124037. [CrossRef]
200. Pseftogkas, A.; Koukouli, M.-E.; Skoulidou, I.; Balis, D.; Meleti, C.; Stavrakou, T.; Falco, L.; Van Geffen, J.; Eskes, H.; Segers, A.; et al. A New Separation Methodology for the Maritime Sector Emissions over the Mediterranean and Black Sea Regions. *Atmosphere* **2021**, *12*, 1478. [CrossRef]
201. Koukouli, M.-E.; Pseftogkas, A.; Karagkiozidis, D.; Skoulidou, I.; Drosoglou, T.; Balis, D.; Bais, A.; Melas, D.; Hatzianastassiou, N. Air Quality in Two Northern Greek Cities Revealed by Their Tropospheric NO₂ Levels. *Atmosphere* **2022**, *13*, 840. [CrossRef]
202. Skoulidou, I.; Koukouli, M.-E.; Segers, A.; Manders, A.; Balis, D.; Stavrakou, T.; Van Geffen, J.; Eskes, H. Changes in Power Plant NO_x Emissions over Northwest Greece Using a Data Assimilation Technique. *Atmosphere* **2021**, *12*, 900. [CrossRef]
203. Zyrichidou, I.; Balis, D.; Koukouli, M.E.; Drosoglou, T.; Bais, A.; Gratsea, M.; Gerasopoulos, E.; Liora, N.; Poupkou, A.; Giannaros, C.; et al. Adverse results of the economic crisis: A study on the emergence of enhanced formaldehyde (HCHO) levels seen from satellites over Greek urban sites. *Atmos. Res.* **2019**, *224*, 42–51. [CrossRef]
204. Vrekoussis, M.; Richter, A.; Hilboll, A.; Burrows, J.P.; Gerasopoulos, E.; Lelieveld, J.; Barrie, L.; Zerefos, C.; Mihalopoulos, N. Economic crisis detected from space: Air quality observations over Athens/Greece. *Geophys. Res. Lett.* **2013**, *40*, 458–463. [CrossRef]
205. Georgoulias, A.K.; Van Der, A.R.J.; Stammes, P.; Boersma, K.F.; Eskes, H.J. Trends and trend reversal detection in 2 decades of tropospheric NO₂ satellite observations. *Atmos. Chem. Phys.* **2019**, *19*, 6269–6294. [CrossRef]
206. Alexandri, G.; Georgoulias, A.K.; Balis, D. Effect of Aerosols, Tropospheric NO₂ and Clouds on Surface Solar Radiation over the Eastern Mediterranean (Greece). *Remote Sens.* **2021**, *13*, 2587. [CrossRef]
207. Koukouli, M.-E.; Skoulidou, I.; Karavias, A.; Parcharidis, I.; Balis, D.; Manders, A.; Segers, A.; Eskes, H.; Van Geffen, J. Sudden changes in nitrogen dioxide emissions over Greece due to lockdown after the outbreak of COVID-19. *Atmos. Chem. Phys.* **2021**, *21*, 1759–1774. [CrossRef]
208. Karagkiozidis, D.; Koukouli, M.-E.; Bais, A.; Balis, D.; Tzoumaka, P. Assessment of the NO₂ Spatio-Temporal Variability over Thessaloniki, Greece, Using MAX-DOAS Measurements and Comparison with S5P/TROPOMI Observations. *Appl. Sci.* **2023**, *13*, 2641. [CrossRef]
209. Drosoglou, T.; Raptis, I.-P.; Valeri, M.; Casadio, S.; Barnaba, F.; Herreras-Giralda, M.; Lopatin, A.; Dubovik, O.; Brizzi, G.; Niro, F.; et al. Evaluating the effects of columnar NO₂ on the accuracy of aerosol optical properties retrievals. *Atmos. Meas. Tech.* **2023**, *16*, 2989–3014. [CrossRef]

210. Georgoulias, A.K.; Papanastasiou, D.K.; Melas, D.; Amiridis, V.; Alexandri, G. Statistical analysis of boundary layer heights in a suburban environment. *Meteorol. Atmos. Phys.* **2009**, *104*, 103–111. [[CrossRef](#)]
211. Kazadzis, S.; Founda, D.; Psiloglou, B.E.; Kambezidis, H.; Mihalopoulos, N.; Sanchez-Lorenzo, A.; Meleti, C.; Raptis, P.I.; Pierros, F.; Nabat, P. Long-term series and trends in surface solar radiation in Athens, Greece. *Atmos. Chem. Phys.* **2018**, *18*, 2395–2411. [[CrossRef](#)]
212. Zerefos, C.S.; Eleftheratos, K.; Meleti, C.; Kazadzis, S.; Romanou, A.; Ichoku, C.; Tselioudis, G.; Bais, A. Solar dimming and brightening over Thessaloniki, Greece, and Beijing, China. *Tellus B Chem. Phys. Meteorol.* **2009**, *61*, 657. [[CrossRef](#)]
213. Bais, A.F.; Drosoglou, T.; Meleti, C.; Tourpali, K.; Kouremeti, N. Changes in surface shortwave solar irradiance from 1993 to 2011 at Thessaloniki (Greece). *Int. J. Climatol.* **2013**, *33*, 2871–2876. [[CrossRef](#)]
214. Natsis, A.; Bais, A.; Meleti, C. Trends from 30-Year Observations of Downward Solar Irradiance in Thessaloniki, Greece. *Appl. Sci.* **2024**, *14*, 252. [[CrossRef](#)]
215. Galanaki, E.; Lagouvardos, K.; Kotroni, V.; Giannaros, T.; Giannaros, C. Implementation of WRF-Hydro at two drainage basins in the region of Attica, Greece, for operational flood forecasting. *Nat. Hazards Earth Syst. Sci.* **2021**, *21*, 1983–2000. [[CrossRef](#)]
216. Alexandri, G.; Georgoulias, A.K.; Meleti, C.; Balis, D.; Kourtidis, K.A.; Sanchez-Lorenzo, A.; Trentmann, J.; Zanis, P. A high resolution satellite view of surface solar radiation over the climatically sensitive region of Eastern Mediterranean. *Atmos. Res.* **2017**, *188*, 107–121. [[CrossRef](#)]
217. Founda, D.; Kazadzis, S.; Mihalopoulos, N.; Gerasopoulos, E.; Lianou, M.; Raptis, P.I. Long-term visibility variation in Athens (1931–2013): A proxy for local and regional atmospheric aerosol loads. *Atmos. Chem. Phys.* **2016**, *16*, 11219–11236. [[CrossRef](#)]
218. Founda, D.; Kalimeris, A.; Pierros, F. Multi annual variability and climatic signal analysis of sunshine duration at a large urban area of Mediterranean (Athens). *Urban. Clim.* **2014**, *10*, 815–830. [[CrossRef](#)]
219. Zerefos, C.; Fountoulakis, I.; Eleftheratos, K.; Kazantzidis, A. Long-term variability of human health-related solar ultraviolet-B radiation doses from the 1980s to the end of the 21st century. *Physiol. Rev.* **2023**, *103*, 1789–1826. [[CrossRef](#)]
220. Bais, A.F.; Zerefos, C.S.; Meleti, C.; Ziomas, I.C.; Tourpali, K. Spectral measurements of solar UVB radiation and its relations to total ozone, SO₂, and clouds. *J. Geophys. Res. Atmos.* **1993**, *98*, 5199–5204. [[CrossRef](#)]
221. Bais, A.F.; McKenzie, R.L.; Bernhard, G.; Aucamp, P.J.; Ilyas, M.; Madronich, S.; Tourpali, K. Ozone depletion and climate change: Impacts on UV radiation. *Photochem. Photobiol. Sci.* **2015**, *14*, 19–52. [[CrossRef](#)]
222. Bais, A.F.; Bernhard, G.; McKenzie, R.L.; Aucamp, P.J.; Young, P.J.; Ilyas, M.; Jöckel, P.; Deushi, M. Ozone—Climate interactions and effects on solar ultraviolet radiation. *Photochem. Photobiol. Sci.* **2019**, *18*, 602–640. [[CrossRef](#)]
223. Meleti, C.; Cappellani, F. Measurements of aerosol optical depth at Ispra: Analysis of the correlation with UV-B, UV-A, and total solar irradiance. *J. Geophys. Res. Atmos.* **2000**, *105*, 4971–4978. [[CrossRef](#)]
224. Campanelli, M.; Diémoz, H.; Siani, A.M.; Di Sarra, A.; Iannarelli, A.M.; Kudo, R.; Fasano, G.; Casasanta, G.; Toffoli, L.; Cacciani, M.; et al. Aerosol optical characteristics in the urban area of Rome, Italy, and their impact on the UV index. *Atmos. Meas. Tech.* **2022**, *15*, 1171–1183. [[CrossRef](#)]
225. Antón, M.; Gil, J.E.; Fernández-Gálvez, J.; Lyamani, H.; Valenzuela, A.; Foyo-Moreno, I.; Olmo, F.J.; Alados-Arboledas, L. Evaluation of the aerosol forcing efficiency in the UV erythemal range at Granada, Spain. *J. Geophys. Res.* **2011**, *116*, D20214. [[CrossRef](#)]
226. Meleti, C.; Bais, A.F.; Kazadzis, S.; Kouremeti, N.; Garane, K.; Zerefos, C. Factors affecting solar ultraviolet irradiance measured since 1990 at Thessaloniki, Greece. *Int. J. Remote Sens.* **2009**, *30*, 4167–4179. [[CrossRef](#)]
227. Raptis, I.-P.; Eleftheratos, K.; Kazadzis, S.; Kosmopoulos, P.; Papachristopoulou, K.; Solomos, S. The Combined Effect of Ozone and Aerosols on Erythemal Irradiance in an Extremely Low Ozone Event during May 2020. *Atmosphere* **2021**, *12*, 145. [[CrossRef](#)]
228. Fountoulakis, I.; Diémoz, H.; Siani, A.M.; di Sarra, A.; Meloni, D.; Sferlazzo, D.M. Variability and trends in surface solar spectral ultraviolet irradiance in Italy: On the influence of geopotential height and lower-stratospheric ozone. *Atmos. Chem. Phys.* **2021**, *21*, 18689–18705. [[CrossRef](#)]
229. Fountoulakis, I.; Redondas, A.; Lakkala, K.; Berjon, A.; Bais, A.F.; Doppler, L.; Feister, U.; Heikkila, A.; Karppinen, T.; Karhu, J.M.; et al. Temperature dependence of the Brewer global UV measurements. *Atmos. Meas. Tech.* **2017**, *10*, 4491–4505. [[CrossRef](#)]
230. Bais, A.F.; Kazadzis, S.; Balis, D.; Zerefos, C.S.; Blumthaler, M. Correcting global solar ultraviolet spectra recorded by a Brewer spectroradiometer for its angular response error. *Appl. Opt.* **1998**, *37*, 6339. [[CrossRef](#)] [[PubMed](#)]
231. Bais, A.F.; Zerefos, C.S.; McElroy, C.T. Solar UVB measurements with the double- and single-monochromator Brewer ozone spectrophotometers. *Geophys. Res. Lett.* **1996**, *23*, 833–836. [[CrossRef](#)]
232. Diémoz, H.; Eleftheratos, K.; Kazadzis, S.; Amiridis, V.; Zerefos, C.S. Retrieval of aerosol optical depth in the visible range with a Brewer spectrophotometer in Athens. *Atmos. Meas. Tech.* **2016**, *9*, 1871–1888. [[CrossRef](#)]
233. Lakkala, K.; Kujanpää, J.; Brogniez, C.; Henriot, N.; Arola, A.; Aun, M.; Auriol, F.; Bais, A.F.; Bernhard, G.; De Bock, V.; et al. Validation of the TROPOspheric Monitoring Instrument (TROPOMI) surface UV radiation product. *Atmos. Meas. Tech.* **2020**, *13*, 6999–7024. [[CrossRef](#)]
234. Arola, A.; Wandji Nyamsi, W.; Lipponen, A.; Kazadzis, S.; Krotkov, N.A.; Tamminen, J. Rethinking the correction for absorbing aerosols in the OMI- and TROPOMI-like surface UV algorithms. *Atmos. Meas. Tech.* **2021**, *14*, 4947–4957. [[CrossRef](#)]
235. Arola, A.; Kazadzis, S.; Krotkov, N.; Bais, A.; Gröbner, J.; Herman, J.R. Assessment of TOMS UV bias due to absorbing aerosols. *J. Geophys. Res. Atmos.* **2005**, *110*, 2005JD005913. [[CrossRef](#)]

236. Zempila, M.M.; Fountoulakis, I.; Taylor, M.; Kazadzis, S.; Arola, A.; Koukouli, M.E.; Bais, A.; Meleti, C.; Balis, D. Validation of OMI erythemal doses with multi-sensor ground-based measurements in Thessaloniki, Greece. *Atmos. Environ.* **2018**, *183*, 106–121. [[CrossRef](#)]
237. Zempila, M.-M.; Van Geffen, J.H.G.M.; Taylor, M.; Fountoulakis, I.; Koukouli, M.-E.; Van Weele, M.; Van Der, A.R.J.; Bais, A.; Meleti, C.; Balis, D. TEMIS UV product validation using NILU-UV ground-based measurements in Thessaloniki, Greece. *Atmos. Chem. Phys.* **2017**, *17*, 7157–7174. [[CrossRef](#)]
238. Kazantzidis, A.; Bais, A.F.; Gröbner, J.; Herman, J.R.; Kazadzis, S.; Krotkov, N.; Kyrö, E.; Den Outer, P.N.; Garane, K.; Görtz, P.; et al. Comparison of satellite-derived UV irradiances with ground-based measurements at four European stations. *J. Geophys. Res. Atmos.* **2006**, *111*, 2005JD006672. [[CrossRef](#)]
239. Zempila, M.-M.; Koukouli, M.-E.; Bais, A.; Fountoulakis, I.; Arola, A.; Kouremeti, N.; Balis, D. OMI/Aura UV product validation using NILU-UV ground-based measurements in Thessaloniki, Greece. *Atmos. Environ.* **2016**, *140*, 283–297. [[CrossRef](#)]
240. Kosmopoulos, P.G.; Kazadzis, S.; Schmalwieser, A.W.; Raptis, P.I.; Papachristopoulou, K.; Fountoulakis, I.; Masoom, A.; Bais, A.F.; Bilbao, J.; Blumthaler, M.; et al. Real-time UV index retrieval in Europe using Earth observation-based techniques: System description and quality assessment. *Atmos. Meas. Tech.* **2021**, *14*, 5657–5699. [[CrossRef](#)]
241. Kosmopoulos, P.G.; Kazadzis, S.; Taylor, M.; Raptis, P.I.; Keramitsoglou, I.; Kiranoudis, C.; Bais, A.F. Assessment of surface solar irradiance derived from real-time modelling techniques and verification with ground-based measurements. *Atmos. Meas. Tech.* **2018**, *11*, 907–924. [[CrossRef](#)]
242. Kosmopoulos, P.; Kazadzis, S.; El-Askary, H.; Taylor, M.; Gkikas, A.; Proestakis, E.; Kontoes, C.; El-Khayat, M. Earth-Observation-Based Estimation and Forecasting of Particulate Matter Impact on Solar Energy in Egypt. *Remote Sens.* **2018**, *10*, 1870. [[CrossRef](#)]
243. Kazantzidis, A.; Nikitidou, E.; Salamatikis, V.; Tzoumanikas, P.; Zagouras, A. New challenges in solar energy resource and forecasting in Greece. *Int. J. Sustain. Energy* **2018**, *37*, 428–435. [[CrossRef](#)]
244. Salamatikis, V.; Vamvakas, I.; Blanc, P.; Kazantzidis, A. Ground-based validation of aerosol optical depth from CAMS reanalysis project: An uncertainty input on direct normal irradiance under cloud-free conditions. *Renew. Energy* **2021**, *170*, 847–857. [[CrossRef](#)]
245. Masoom, A.; Kosmopoulos, P.; Bansal, A.; Kazadzis, S. Solar Energy Estimations in India Using Remote Sensing Technologies and Validation with Sun Photometers in Urban Areas. *Remote Sens.* **2020**, *12*, 254. [[CrossRef](#)]
246. Masoom, A.; Kosmopoulos, P.; Bansal, A.; Gkikas, A.; Proestakis, E.; Kazadzis, S.; Amiridis, V. Forecasting dust impact on solar energy using remote sensing and modeling techniques. *Sol. Energy* **2021**, *228*, 317–332. [[CrossRef](#)]
247. Nikitidou, E.; Kazantzidis, A.; Salamatikis, V. The aerosol effect on direct normal irradiance in Europe under clear skies. *Renew. Energy* **2014**, *68*, 475–484. [[CrossRef](#)]
248. Kosmopoulos, P.G.; Kazadzis, S.; Taylor, M.; Athanasopoulou, E.; Speyer, O.; Raptis, P.I.; Marinou, E.; Proestakis, E.; Solomos, S.; Gerasopoulos, E.; et al. Dust impact on surface solar irradiance assessed with model simulations, satellite observations and ground-based measurements. *Atmos. Meas. Tech.* **2017**, *10*, 2435–2453. [[CrossRef](#)]
249. Kouklaki, D.; Kazadzis, S.; Raptis, I.-P.; Papachristopoulou, K.; Fountoulakis, I.; Eleftheratos, K. Photovoltaic Spectral Responsivity and Efficiency under Different Aerosol Conditions. *Energy* **2023**, *16*, 6644. [[CrossRef](#)]
250. Kambezidis, H.D. The Solar Radiation Climate of Greece. *Climate* **2021**, *9*, 183. [[CrossRef](#)]
251. Nikitidou, E.; Kazantzidis, A.; Tzoumanikas, P.; Salamatikis, V.; Bais, A.F. Retrieval of surface solar irradiance, based on satellite-derived cloud information, in Greece. *Energy* **2015**, *90*, 776–783. [[CrossRef](#)]
252. Zempila, M.-M.; Giannaros, T.M.; Bais, A.; Melas, D.; Kazantzidis, A. Evaluation of WRF shortwave radiation parameterizations in predicting Global Horizontal Irradiance in Greece. *Renew. Energy* **2016**, *86*, 831–840. [[CrossRef](#)]
253. Bais, A. Hellenic Network for Solar Energy BT—Advances in Meteorology. In *Climatology and Atmospheric Physics*; Springer Atmospheric Sciences; Springer: Berlin/Heidelberg, Germany, 2012. [[CrossRef](#)]
254. Zagouras, A.; Kazantzidis, A.; Nikitidou, E.; Argiriou, A.A. Determination of measuring sites for solar irradiance, based on cluster analysis of satellite-derived cloud estimations. *Sol. Energy* **2013**, *97*, 1–11. [[CrossRef](#)]
255. Nikitidou, E.; Zagouras, A.; Salamatikis, V.; Kazantzidis, A. Short-term cloudiness forecasting for solar energy purposes in Greece, based on satellite-derived information. *Meteorol. Atmos. Phys.* **2019**, *131*, 175–182. [[CrossRef](#)]
256. Tzoumanikas, P.; Nikitidou, E.; Bais, A.F.; Kazantzidis, A. The effect of clouds on surface solar irradiance, based on data from an all-sky imaging system. *Renew. Energy* **2016**, *95*, 314–322. [[CrossRef](#)]
257. Raptis, P.I.; Kazadzis, S.; Psiloglou, B.; Kouremeti, N.; Kosmopoulos, P.; Kazantzidis, A. Measurements and model simulations of solar radiation at tilted planes, towards the maximization of energy capture. *Energy* **2017**, *130*, 570–580. [[CrossRef](#)]
258. Kambezidis, H.D.; Psiloglou, B.E. Estimation of the Optimum Energy Received by Solar Energy Flat-Plate Convertors in Greece Using Typical Meteorological Years. Part I: South-Oriented Tilt Angles. *Appl. Sci.* **2021**, *11*, 1547. [[CrossRef](#)]
259. Kosmopoulos, P.; Kouroutsidis, D.; Papachristopoulou, K.; Raptis, P.I.; Masoom, A.; Saint-Drenan, Y.-M.; Blanc, P.; Kontoes, C.; Kazadzis, S. Short-Term Forecasting of Large-Scale Clouds Impact on Downwelling Surface Solar Irradiation. *Energy* **2020**, *13*, 6555. [[CrossRef](#)]
260. Kosmopoulos, P.G.; Kazadzis, S.; Lagouvardos, K.; Kotroni, V.; Bais, A. Solar energy prediction and verification using operational model forecasts and ground-based solar measurements. *Energy* **2015**, *93*, 1918–1930. [[CrossRef](#)]
261. Available online: https://solar.beyond-eocenter.eu/#solar_short (accessed on 22 June 2014).

262. Raptis, I.-P.; Kazadzis, S.; Fountoulakis, I.; Papachristopoulou, K.; Kouklaki, D.; Psiloglou, B.E.; Kazantzidis, A.; Benetatos, C.; Papadimitriou, N.; Eleftheratos, K. Evaluation of the Solar Energy Nowcasting System (SENSE) during a 12-Months Intensive Measurement Campaign in Athens, Greece. *Energy* **2023**, *16*, 5361. [[CrossRef](#)]
263. Papachristopoulou, K.; Fountoulakis, I.; Bais, A.F.; Psiloglou, B.E.; Papadimitriou, N.; Raptis, I.-P.; Kazantzidis, A.; Kontoes, C.; Hatzaki, M.; Kazadzis, S. Effects of clouds and aerosols on downwelling surface solar irradiance nowcasting and short-term forecasting. *Atmos. Meas. Tech. Discuss.* **2023**, *2023*, 1–31. [[CrossRef](#)]
264. World Meteorological Organization Instruments and Observing Methods The WMO Automatic Digital Barometer Intercomparison; Published by WMO. 1992. Available online: <https://library.wmo.int/idurl/4/41750> (accessed on 22 May 2024).
265. Founda, D.; Nastos, P.T.; Pierros, F.; Kalimeris, A. Historical observations of cloudiness (1882–2012) over a large urban area of the eastern Mediterranean (Athens). *Appl. Clim.* **2019**, *137*, 283–295. [[CrossRef](#)]
266. Hamilton, D.S.; Moore, J.K.; Arneth, A.; Bond, T.C.; Carslaw, K.S.; Hantson, S.; Ito, A.; Kaplan, J.O.; Lindsay, K.; Nieradzik, L.; et al. Impact of Changes to the Atmospheric Soluble Iron Deposition Flux on Ocean Biogeochemical Cycles in the Anthropocene. *Glob. Biogeochem. Cycles* **2020**, *34*, e2019GB006448. [[CrossRef](#)]
267. Ito, A.; Ye, Y.; Baldo, C.; Shi, Z. Ocean fertilization by pyrogenic aerosol iron. *NPJ Clim. Atmos. Sci.* **2021**, *4*, 30. [[CrossRef](#)]
268. Myriokefalitakis, S.; Gröger, M.; Hieronymus, J.; Döscher, R. An explicit estimate of the atmospheric nutrient impact on global oceanic productivity. *Ocean Sci.* **2020**, *16*, 1183–1205. [[CrossRef](#)]
269. Ito, A.; Myriokefalitakis, S.; Kanakidou, M.; Mahowald, N.M.; Scanza, R.A.; Hamilton, D.S.; Baker, A.R.; Jickells, T.; Sarin, M.; Bikkina, S.; et al. Pyrogenic iron: The missing link to high iron solubility in aerosols. *Sci. Adv.* **2019**, *5*, eaau7671. [[CrossRef](#)]
270. Rathod, S.D.; Hamilton, D.S.; Mahowald, N.M.; Klimont, Z.; Corbett, J.J.; Bond, T.C. A Mineralogy-Based Anthropogenic Combustion-Iron Emission Inventory. *J. Geophys. Res. Atmos.* **2020**, *125*, e2019JD032114. [[CrossRef](#)]
271. Wang, T.; Hendrick, F.; Wang, P.; Tang, G.; Clément, K.; Yu, H.; Fayt, C.; Hermans, C.; Gielen, C.; Müller, J.-F.; et al. Evaluation of tropospheric SO₂ retrieved from MAX-DOAS measurements in Xianghe, China. *Atmos. Chem. Phys.* **2014**, *14*, 11149–11164. [[CrossRef](#)]
272. Myriokefalitakis, S.; Nenes, A.; Baker, A.R.; Mihalopoulos, N.; Kanakidou, M. Bioavailable atmospheric phosphorous supply to the global ocean: A 3-D global modeling study. *Biogeosciences* **2016**, *13*, 6519–6543. [[CrossRef](#)]
273. Kanakidou, M.; Duce, R.A.; Prospero, J.M.; Baker, A.R.; Benitez-Nelson, C.; Dentener, F.J.; Hunter, K.A.; Liss, P.S.; Mahowald, N.; Okin, G.S.; et al. Atmospheric fluxes of organic N and P to the global ocean. *Glob. Biogeochem. Cycles* **2012**, *26*, 2011GB004277. [[CrossRef](#)]
274. Hamilton, D.S.; Perron, M.M.G.; Bond, T.C.; Bowie, A.R.; Buchholz, R.R.; Guieu, C.; Ito, A.; Maenhaut, W.; Myriokefalitakis, S.; Olgun, N.; et al. Earth, Wind, Fire, and Pollution: Aerosol Nutrient Sources and Impacts on Ocean Biogeochemistry. *Ann. Rev. Mar. Sci.* **2022**, *14*, 303–330. [[CrossRef](#)]
275. Myriokefalitakis, S.; Daskalakis, N.; Mihalopoulos, N.; Baker, A.R.; Nenes, A.; Kanakidou, M. Changes in dissolved iron deposition to the oceans driven by human activity: A 3-D global modelling study. *Biogeosciences* **2015**, *12*, 3973–3992. [[CrossRef](#)]
276. Kanakidou, M.; Myriokefalitakis, S.; Tsagkaraki, M. Atmospheric inputs of nutrients to the Mediterranean Sea. *Deep Sea Res. Part II Top. Stud. Oceanogr.* **2020**, *171*, 104606. [[CrossRef](#)]
277. Nenes, A.; Krom, M.D.; Mihalopoulos, N.; Van Cappellen, P.; Shi, Z.; Bougiatioti, A.; Zarmpas, P.; Herut, B. Atmospheric acidification of mineral aerosols: A source of bioavailable phosphorus for the oceans. *Atmos. Chem. Phys.* **2011**, *11*, 6265–6272. [[CrossRef](#)]
278. Violaki, K.; Tsiodra, I.; Nenes, A.; Tsagkaraki, M.; Kouvarakis, G.; Zarmpas, P.; Florou, K.; Panagiotopoulos, C.; Ingall, E.; Weber, R.; et al. Water soluble reactive phosphate (SRP) in atmospheric particles over East Mediterranean: The importance of dust and biomass burning events. *Sci. Total Environ.* **2022**, *830*, 154263. [[CrossRef](#)]

Disclaimer/Publisher’s Note: The statements, opinions and data contained in all publications are solely those of the individual author(s) and contributor(s) and not of MDPI and/or the editor(s). MDPI and/or the editor(s) disclaim responsibility for any injury to people or property resulting from any ideas, methods, instructions or products referred to in the content.